Structural evidence for a [4Fe-5S] intermediate in the non-redox desulfuration of thiouracil

Jingjing Zhou, Ludovic Pecqueur, Agota Aučynaitė, Jonathan Fuchs, Rasa Rutkienė, Justas Vaitekūnas, Rolandas Meškys, Matthias Boll, Marc Fontecave, Jaunius Urbonavičius, et al.

Structural evidence for a [4Fe-5S] intermediate in the non-redox desulfuration of thiouracil

Authors: Jingjing Zhou[1⊥], Ludovic Pecqueur[1⊥], Agota Aučynaitė[2], Jonathan Fuchs[3], Rasa Rutkienė[2], Justas Vaitekūnas[2], Rolandas Meškys[2], Matthias Boll[3], Marc Fontecave[1], Jaunius Urbonavičius[2,4*], Béatrice Golinelli-Pimpaneau[1*]

Affiliations:

[1] Laboratoire de Chimie des Processus Biologiques, UMR 8229 CNRS, Collège de France, Sorbone Université, Paris CEDEX 05, France.

[2] Department of Molecular Microbiology and Biotechnology, Institute of Biochemistry, Life Sciences Center, Vilnius University, Vilnius, Lithuania.

[3] Faculty of Biology - Microbiology, University of Freiburg, 79104, Freiburg, Germany.

[4] Department of Chemistry and Bioengineering, Vilnius Gediminas Technical University, Vilnius, Lithuania.

* Correspondence: beatrice.golinelli@college-de-france, jaunius.urbonavicius@vgtu.lt
[⊥]Co-1st authors

ABSTRACT

We recently discovered a [Fe-S]-containing protein with *in vivo* **t**hio**u**racil **d**e**s**ulfidase activity called TudS. We report here the crystal structure of TudS, refined at 1.5 Å resolution, which harbors a [4Fe-4S] cluster, bound by three cysteines only. Incubation of TudS crystals with 4-thiouracil trapped the cluster with a hydrosulfide ligand bound to the fourth non-protein-bonded iron, as established by the sulfur anomalous signal. This indicates that a [4Fe-5S] state of the cluster is a catalytic intermediate in the desulfuration reaction. Structural data and site-directed mutagenesis indicate that a water molecule is located next to the hydrosulfide ligand and to two catalytically important residues, Ser101 and Glu45. This information together with modeling studies allow us to propose a mechanism for the unprecedented nonredox enzymatic desulfuration of thiouracil, in which a [4Fe-4S] cluster binds and activates the sulfur atom of the substrate.

INTRODUCTION

A large number of important biological compounds contain one or several sulfur atoms. These molecules include organic cofactors such as thiamin, molybdopterin, biotin or lipoic acid, inorganic cofactors such as the various classes of iron-sulfur clusters and a variety of thionucleosides present in tRNAs [1]. During the last 20 years, tremendous efforts have aimed at discovering the enzymes responsible for the sulfuration reactions involved in the biosynthesis of these compounds and at understanding the mechanisms of sulfur transfer from the sulfur donor to the sulfur acceptor [2-5]. The general agreement is that, due to its toxicity, sulfur is stored in the cell in the form of L-cysteine. In most cases, pyridoxal-phosphate-dependent L-cysteine desulfurases liberate sulfur from L-cysteine in the form of protein-bound persulfides which, through trans-persulfuration reactions, provide the sulfur atoms to the final biosynthetic enzyme [6]. However, an emerging class of sulfur transferases was recently shown to depend on a catalytically active [4Fe-4S] cluster for redox reactions, as in the case of lipoate and biotin synthases [7-10] and also for non-redox reactions, as in the case of thiocytidine and thiouridine synthesis in tRNAs [11-14]. The presence of sulfur atoms within the cluster prompts to question whether the sulfur transferase could use these « internal » S atoms as a source of sulfur for the sulfuration reaction (Scheme 1A).

Scheme 1. Scheme Title: [4Fe-4S] clusters can either give or receive a sulfur atom for sulfuration reactions. **A** In the case of biotin or lipoate synthesis, a [4Fe-4S] cluster yields one sulfur atom to the substrate to form a [4Fe-3S] cluster and the sulfurated product. **B** In the case of thiocytidine or thiouridine synthesis in tRNA, a [4Fe-4S] cluster receives a sulfur atom, forming a [4Fe-5S] cluster, and gives it to the substrate to form the sulfurated product.

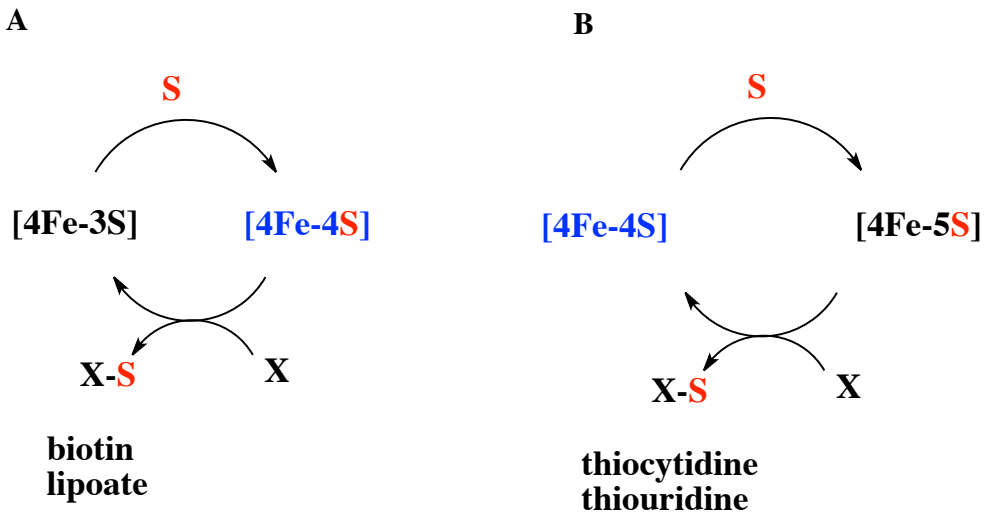

Such mechanism, which implies that the cluster is partly destroyed and repaired during catalysis, and thus that the enzyme cycles between a [4Fe-3S] state and an active [4Fe-4S] state (Scheme 1A), has been proposed for biotin or lipoate synthesis, catalyzed by the BioB and LipA enzymes, respectively [7-10]. In contrast, for thiouridine or thiocytidine synthesis during tRNA modification, catalyzed by TtuA [12-14] and TtcA [11], respectively, we and others proposed a mechanism (Figure 1b), in which the cluster remains intact during catalysis and proceeds via binding of an « external » S atom to one of the 4 Fe atoms, leading to a putative [4Fe-5S] cluster intermediate, from which the activated S atom is then transferred to the substrate. In these enzymes, only three Fe atoms of the cluster are bound to a cysteine of the protein, while the

fourth Fe has a free coordination site that enables binding of exogenous ligands and cycling of the enzyme between a [4Fe-4S] state and an active [4Fe-5S] state.
Here we study a [4Fe-4S]-containing enzyme that promotes the direct transfer of a sulfur atom from its sulfurated substrate to the [4Fe-4S] cluster, unambiguously characterize the product as a [4Fe-5S] cluster by high-resolution X-ray crystallography and propose a mechanism for its formation. This enzyme catalyzes efficient desulfuration of thiouracil to uracil and was identified following the recent discovery of novel genes encoding proteins from the Domain of Unknown function 523 (DUF523) family [15]. The present work provides a strong support to a novel function of iron-sulfur clusters in biology, namely as sulfur transfer agents.

RESULTS

TudS is a [4Fe-4S] containing enzyme that converts 2-thiouracil and 4-thiouracil into uracil

Several DUF523 genes have previously been characterized as ORFs that could complement growth of an *E. coli* uracil auxotroph strain in the presence of 2-thiouracil [15], thus showing that the encoded protein family has the ability to catalyze *in vivo* 2-thiouracil desulfuration into uracil. Here, we thus name these enzymes TudS for **t**hio**u**racil **d**e**s**ulfidase. Figure S1 displays the amino acid sequences of a few TudS proteins. One of them, originating from an *Aeromonas* species, has previously been partially purified [15]. It exhibited a UV-visible spectrum with an absorption band at around 420 nm, suggesting the presence of a [Fe-S] cluster. Yet, the chemical nature of the cluster could not be defined solely based on this spectrum and its role in catalysis was not established. As shown in Figure S2, the *in vivo* 2-thiouracil sulfuration activity of TudS is confirmed here. Furthermore, 2-thiouracil can be replaced by 4-thiouracil to complement the uracil auxotrophic strain, indicating that the latter is also a substrate of TudS.

Our goal was to decipher the chemical mechanism of TudS enzymes. We thus first purified the TudS protein from *Aeromonas* aerobically to near homogeneity (Figure S3A). As expected for an enzyme containing an oxygen-sensitive [Fe-S] cluster, only residual amounts of Fe and S were found within the as-purified protein. In order to get the protein in the holo-form, reconstitution of the [Fe-S] cluster was then carried out *in vitro* under strict anaerobic conditions by treating as-purified TudS with ferrous iron and a biochemical source of sulfide, consisting of L-cysteine and a cysteine desulfurase CsdA, in the presence of DTT. After purification on a Superdex 200 gel filtration column under anaerobic conditions, a homogenous brownish solution containing the holo-TudS protein was obtained (Figure S3B). SEC-MALS analysis indicated that holo-TudS is a monomer in solution (Figure S3C). Iron and labile sulfur were quantified using the Beinert and Fish methods [16, 17]. Holo-TudS contained 3.8 ± 0.3 Fe and 3.1± 0.8 S per monomer and its UV-visible spectrum displayed an absorption band at around 410 nm characteristic of the presence of a $[4Fe\text{-}4S]^{2+}$ cluster (Figure S3D). Altogether, these data support the presence of one [4Fe-4S] cluster with almost full occupancy in holo-TudS after cluster reconstitution.
The desulfuration activity of purified holo-TudS towards 2-thiouracil and 4-thiouracil was monitored *in vitro* by following the formation of the uracil product after separation on a reversed phase chromatography column (Figure S4). Because 4-thiouracil was converted faster than 2-thiouracil, it appears that the enzyme preferentially abstracts sulfur at position 4 rather than position 2.

The crystal structure of TudS shows a [4Fe-4S] cluster with only three cysteine ligands

We crystallized TudS in space group C2 (Table S1A) with two molecules in the asymmetric unit (Figure S5A) that differ only in their N- and C-terminal extremities (Figure S5B). Analysis

of the interface between the two molecules in the asymmetric unit using *PISA* [18] did not reveal any specific interactions that could result in the formation of stable quaternary structures, in agreement with TudS being a monomer in solution (Figure S3C).
The crystal structure unambiguously shows that holo-TudS contains a [4Fe-4S] cubane cluster, which is bound by three cysteines only (Cys10, Cys43 and Cys104) (Figure 1A).

Figure 1. Figure Title : Crystallographic structure of TudS after cluster reconstitution. **A** Overall architecture of TudS. Three conserved cysteines (Cys10, Cys43 and Cys104) are bound to three iron atoms of the [4Fe-4S] cluster, while the fourth iron atom is bound to the two oxygen atoms of an ethylene glycol (EDO) molecule present in the cryoprotectant solution. Fe and S atoms are shown as orange and yellow spheres, respectively. **B** Anomalous difference map for sulfur (data collected at 6.5 keV; PDB code 6Z94) contoured at 3.5 σ, showing that anomalous signal is observed only for the sulfur atoms of the [4Fe-4S] cluster and the cysteine ligands. **C** Hydrogen bonding interactions within 3.2 Å near the [4Fe-4S] cluster and the ethylene glycol ligand. **D** Electrostatic surface calculated with APBS and displayed within +/- 5kTe^{-1}. The ethylene glycol molecule blocks access to the cluster, which is buried within the structure. The entry to the active site consists of an extended positively charged surface (~640 Å^2).

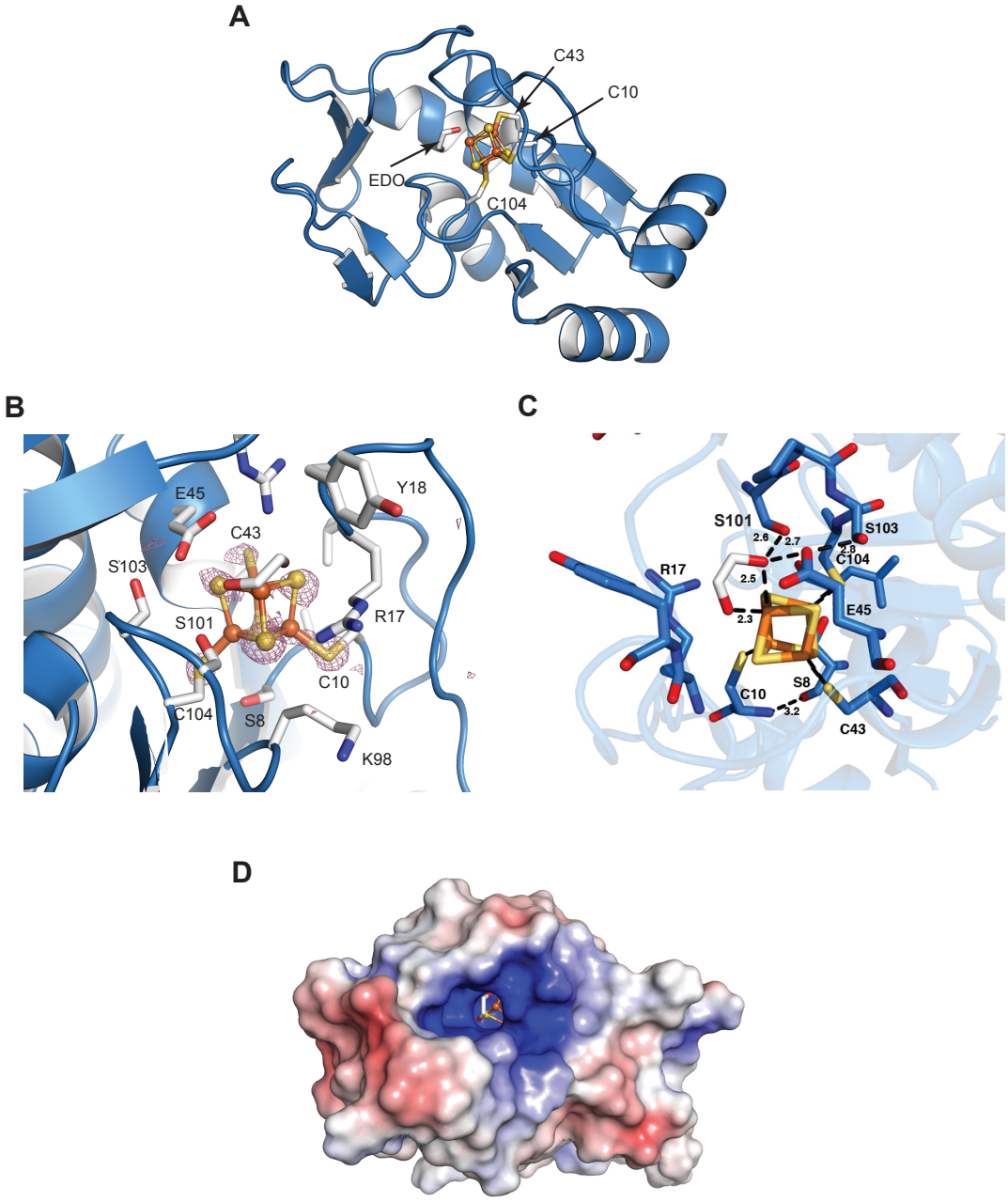

These cysteines are fully conserved (Figure S1) and had previously been shown to be essential for activity, using the *in vivo* complementation assay [15]. A clear electron density near the

fourth, non-protein-bonded, iron atom was observed and assigned to ethylene glycol, which was used as a cryoprotectant agent (Figure S5C & Figure 1). The two hydroxyl groups of ethylene glycol are located 2.3 and 2.5 Å away from the fourth iron atom (Figure 1C), indicating that the fourth Fe atom is penta-coordinated. In addition, one ethylene glycol hydroxyl group makes hydrogen-bonding interactions to Ser101 OG and Glu45 OE2, the position of which is also maintained by a hydrogen bond with the Ser103 OG atom. The ligand blocks solvent access to the [4Fe-4S] cluster (Figure 1D) and is located at the bottom of an 840 $Å^3$ cavity, which includes Arg17, Lys23 and Lys98 (Figure 1B) and is mostly positively charged, as shown by the electrostatic surface calculated using APBS [19] (Figure 1D).

A [4Fe-5S] cluster is formed upon soaking TudS crystals with the 4-thiouracil substrate. In order to get further insight into the chemistry of the enzymatic reaction, we aimed at obtaining the structure of TudS in complex with substrates or catalytic intermediates. Several TudS crystals were therefore incubated in the presence of 4-thiouracil substrate (15 mM) for 5-15 min, then soaked in a cryoprotectant solution before freezing in propane. X-ray diffraction data were collected at 6.5 and 7.125 keV for sulfur and iron detection, respectively (Table S1B; Figure S6A). Compared to the non-soaked crystals (Figures 1B & S5C), no density corresponding to ethylene glycol nor 4-thiouracil was observed (Figure 2A).

Figure 2. Figure Title: Crystallographic structure of the [4Fe-5S] cluster of TudS (crystal 4 soaked for 5 minutes with 15 mM 4-thiouracil, molecule A). **A** Anomalous difference map for sulfur (data collected at 6.5 keV) contoured at 3.5 σ obtained for TudS. An additional anomalous signal labeled as "S" is detectable near the fourth iron of the cluster, indicating binding of a hydrosulfide ligand and formation of a [4Fe-5S] cluster. A weak anomalous signal is also detected for the Fe atoms. In addition, a water molecule, indicated as a green sphere, is also bound to the fourth iron atom of the cluster. **B** Hydrogen bonding interactions within 3.2 Å near the [4Fe-45] cluster and the water molecule.

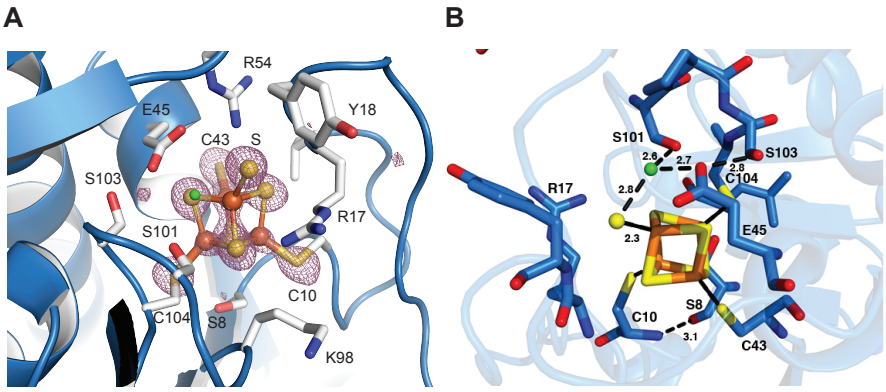

In contrast, additional anomalous signal was visible near the fourth iron of the cluster after soaking crystals with 15 mM thiouracil for 5 min (Figures 2A & S6A). This anomalous contribution, centered 2.3 Å away from the iron atom, was similar to that of the sulfur atoms of the [4Fe-4S] cluster and the cysteine ligands, clearly indicating that the ligand bound to the [4Fe-4S] cluster is hydrosulfide and that a [4Fe-5S] cluster was formed. Importantly, the sulfur anomalous signals near the fourth iron atom were present in the two molecules of the crystal soaked with thiouracil but NOT in the non-soaked crystal, indicating that the fifth sulfur atom of the [4Fe-5S] cluster came from 4-thiouracil and that, therefore, the protein catalyzed desulfuration of 4-thiouracil within the crystal *via* sulfur transfer to the cluster and generation of a [4Fe-5S] cluster.

A careful analysis of the density maps of the soaked crystals indicated small differences between molecules A and B. In molecule A, the fourth iron atom is bound to an external sulfur ligand, which is located 2.8 Å away from a water molecule (Figure 2A & 2B). This water molecule is also located 2.9 Å away from the fourth iron atom, a too long distance for a covalent bond, and is in hydrogen bond distance with the Ser101 OG and the Glu45 OE2 atoms (Figure 2B). In contrast, in molecule B, the fifth S atom occupies two positions: one, with the higher occupancy, is identical to that in molecule A, while the other, with the lower occupancy, corresponds approximately to that occupied by the water molecule in molecule A (Figures S6B & S6C). These two positions are comparable to those of the two hydroxyl groups of the ethylene glycol ligand in the non-soaked crystal (Figure 1C). Altogether, all these data point to the presence of two sites near the cluster that can be occupied by sulfur or oxygen atoms from exogenous ligands.

To analyze in more detail the conformations adopted by the [4Fe-5S] cluster of TudS, we calculated the angles formed by each Fe-S bond within the cluster with the bond linking the Fe atom and the external hydrosulfide ligand (Figure S7). Then, we examined the structures of [4Fe-4S]-containing proteins in the protein data bank (PDB), solved at a resolution better than 1.45 Å resolution, and measured the angles formed between each Fe-S bond of the cluster (the S atom belonging the cluster) with the bond linking the Fe atom and its sulfur-containing ligand (the S atom being external to the cluster) (Figure S8). In standard [4Fe-4S] clusters, the external S-containing ligand is most often a L-cysteine. By comparison, the angles in both conformations of the [4Fe-5S] cluster of TudS are significantly different than those observed in other structures (Figure S8). Interestingly, the non-catalytic β-subunit of 2-hydroxyisocaproyl-CoA dehydratase (HadC) [20] also possesses a [4Fe-4S] bound to a hydrosulfide ligand, while another enzyme named DCCP (double-cubane cluster protein) was found to house a double-cubane type [8Fe-9S]-cluster i. e. two [4Fe-4S] clusters bridged by a μ_2-S ligand [21]. The clusters of HadC and DCCP, which are the most relevant for comparison with TudS, have a geometry similar to that observed in standard structures, not to that found in TudS (Figures S7 & S8; Table S2). Therefore, we estimate that the fifth sulfur atom of the [4Fe-5S] cluster of TudS enjoys specific constraints that result in a specific geometry that might be important for the catalytic reactivity of the enzyme.

The TudS structure displays the highest structural homology with [4Fe-4S]-dependent 2-hydroxyisocaproyl-CoA dehydratase

A survey of the PDB using DaliLite v.5 (http://ekhidna2.biocenter.helsinki.fi/dali/) [22] indicates that TudS does not show strong matches with proteins from the PDB (a strong match being defined by a Z-score > (n/10) − 4, with n the number of residues, i.e. Z-score > 11.3 for TudS that contains 153 residues). Interestingly, the highest structural homology was found with HadC [20] (Z score = 6.6, rmsd of 3 Å for 93 atoms). TudS is much shorter in sequence than 2-hydroxyisocaproyl-CoA dehydratase and superposition of TudS with its β-subunit HadC shows that it is similar only to its C-terminal domain (Figure S9A). Interestingly, after superposition, the location of the clusters of both proteins is similar, indicating that both proteins adopt a similar fold to bind a [4Fe-4S] cluster. Outstandingly, a [4Fe-5S] cluster was observed in the crystal structures of both TudS and HadC. Yet, the cavity corresponding to the HadC cluster is buried and shielded from bulk solvent [20], whereas the fifth sulfur atom of TudS is located at the bottom of a channel that extends towards the solvent (Figure S9B).

Site-directed mutagenesis reveals that Ser101 and Glu45 are crucial catalytic residues

The active site structure highlights several residues positioned near the cluster that are likely to have a catalytic function. We thus mutated Arg17, Tyr18, Glu45, Lys98, Ser101 and Ser103, residues located in the vicinity of the [4Fe-4S] cluster (Figure 1B) that are conserved among potential TudS proteins from various organisms (Figure S1). The TudS variants were tested for the loss of *in vivo* thiouracil desulfuration activity by monitoring growth complementation of the *E. coli* uracil auxotroph on minimal medium using 2-thiouracil or 4-thiouracil as sources of uracil (Table 1 and Figure S2).

Table 1. *In vivo* activity of TudS mutants monitored by complementation of the *E. coli* HMS174Δ*pyrF* strain. 2-thiouracil and 4-thiouracil were used as sources of uracil in the minimal M9 medium. See complementary information in Figure S2.

TudS mutant	2-Thiouracil	4-Thiouracil
R17A	+	+
R17K	+	+
R17M	+	+
Y18A	+	+
Y18F	+	+
Y18L	+	+
E45A	**-**	**-**
E45D	**+**	**+**
E45Q	**-**	**-**
K98A	+	+
K98L	+	+
S101A	**-**	**-**
S101C	**-**	**-**
S101T	**-**	**+**
S103A	**+**	**+**
S103C	**-**	**+**
S103T	**+**	**+**

"+" indicates mutants that complemented the growth of *E. coli* uracil auxotroph HMS174Δ*pyrF* on minimal M9 medium and "-" mutants that do not.

Mutations of Arg17, Tyr18 and Lys98 had no effect on activity, indicating that they are not directly involved in the catalytic mechanism. Ser103 does not appear to have a crucial role for catalysis because the S103A and S103T mutants could complement the auxotrophic strain. Yet, interestingly, the S103C mutant could complement the auxotrophic strain when using 4-thiouracil as the substrate, but not when using 2-thiouracil. This suggests that Ser103 might help desulfurate 2-thiouracil, but not 4-thiouracil. The carboxylate of Glu45 seems to be critical since mutation of this residue into alanine or glutamine resulted into an inactive enzyme while the E45D mutant could complement the uracil auxotrophic strain. Similarly, the hydroxyl group of Ser101 is essential since the S101A and S101C mutants could not complement the uracil auxotrophic strain, while the S101T could do it, however only with 4-thiouracil as a substrate. A correct positioning of the hydroxyl group of Ser101 is thus crucial for desulfuration of 2-thiouracil, whereas less accuracy is required for the desulfuration of 4-thiouracil. Altogether, the mutagenesis results indicate that Ser101 and Glu45 appear to be the critical catalytic residues.

Models for thiouracil-TudS complexes

To gain insight into the structure of the enzyme/substrate complexes, the 2-thiouracil and 4-thiouracil substrates were docked into the TudS structure using the EADock program, provided by the Swissdock web server [23]. This program, dedicated to the blind docking of small molecules on target proteins, samples the dominant conformations of the ligand into clusters. The protein-ligand binding energy is evaluated using a scoring function based on the CHARMM22 force field. We analyze here the models of lowest energy obtained without constraining the docking, in which, interestingly, the thiol group of the substrates is located near the [4Fe-4S] cluster of TudS (Figure S10 & Table S3).
For both thiouracil substrates, the lowest energy corresponds to the conformation with the sulfur located less than 2.5 Å away from the non-protein bonded Fe atom of the cluster, consistent with a covalent bond, despite the wide space sampling of the docking, indicating very specific binding of the ligand to TudS. 2-thiouracil and 4-thiouracil could be docked equally well at the TudS cluster site, according to the free energy of interaction ΔG. Two conformations of similar energies were found, with the rings rotated 180° relative to each other along the C-S bond axis (Figure S10). In all of them, the uracil base is sandwiched between Tyr18 and Pro102 and in most of them the N1 or N3 atom makes a hydrogen bond with the Glu45 OE1 atom. In the models, the C-S bond is located near the Glu45 OE1 and Ser101 OG1 atoms (Table S3), confirming that these residues could play a crucial role in catalysis.

DISCUSSION

Our recent discovery of a class of enzymes involved in desulfuration of thiouracil and conversion into uracil is intriguing [15]. Indeed, very few studies so far have reported the presence of free thiouracil compounds within cells. Furthermore, while the potential toxicity of thiouracil was mentioned in the literature [24, 25], there are also reports showing beneficial effects of thiouracil diet complementation [26, 27]. Nevertheless, the discovery of TudS indicates a need for cells to promote this reaction, either for limiting cellular concentration of thiouracil, participate in a salvage pathway for uracil synthesis [28] or as a way to mobilize the sulfur atom of thiouracil for a still-unknown way of utilization of the sulfur atom. This opens an interesting field of research within the general field of cellular sulfur metabolism that is still incompletely established.
From a biochemical point of view, this work provides the first detailed characterization of TudS. In particular, while preliminary results suggested the presence of an iron-sulfur cluster, the crystal structure of TudS reported here unambiguously shows the presence of a [4Fe-4S] cluster chelated by only three cysteines, leaving the fourth iron atom available for coordinating exogenous ligands. In the present case, an ethylene glycol molecule derived from the crystallization medium occupies the free coordination site. The cysteine residues at positions 10, 43 and 104, provide the other, protein-derived, ligands to the cluster. Because previous site-directed mutagenesis of TudS had shown that these cysteines are essential for *in vivo* enzymatic activity of TudS [15], altogether, the mutagenesis and crystallographic data indicate that the [4Fe-4S] cluster is essential for catalysis.
An important outcome of this study is the finding that TudS catalyzes the abstraction of the sulfur atom of thiouracil and its transfer to the cluster, where it ends up bound to the fourth Fe atom. This reaction occured *in crystallo,* during anaerobic soaking of thiouracil into a crystal of TudS. A "stable" [4Fe-5S] cluster was formed, whose structure was determined by X-ray crystallography. The presence of the exogenous S atom was unambiguously identified by its anomalous contribution at 6.5 keV.
In this work, the docking of 2-thiouracil and 4-thiouracil into the TudS structure has shown that both molecules can bind deeply in the pocket, near the [4Fe-4S] cluster. Moreover, in the most stable structures of the complexes, the thiouracil substrates bind to the cluster *via* a bond

between their S atom and the fourth unique iron. Altogether, the crystal structure of TudS, combined with modeling studies of TudS-thiouracil complexes and site-directed mutagenesis, allow us to propose a mechanism for desulfuration of the 4-thiouracil substrate by TudS (Figure 3).

Figure 3. Figure Title: Proposed reaction mechanism for 4-thiouracil desulfuration by TudS involving the formation of a [4Fe-5S] intermediate. **A** Model of the 4-thiouracil/TudS complex. **B** Crystal structure of the [4Fe-5S] intermediate. **C** Proposed catalytic mechanism of TudS. Catalysis is probably assisted by two active site bases that can be assigned to Glu45 and Ser101 based on the crystal structure of TudS, docking and mutagenesis data.

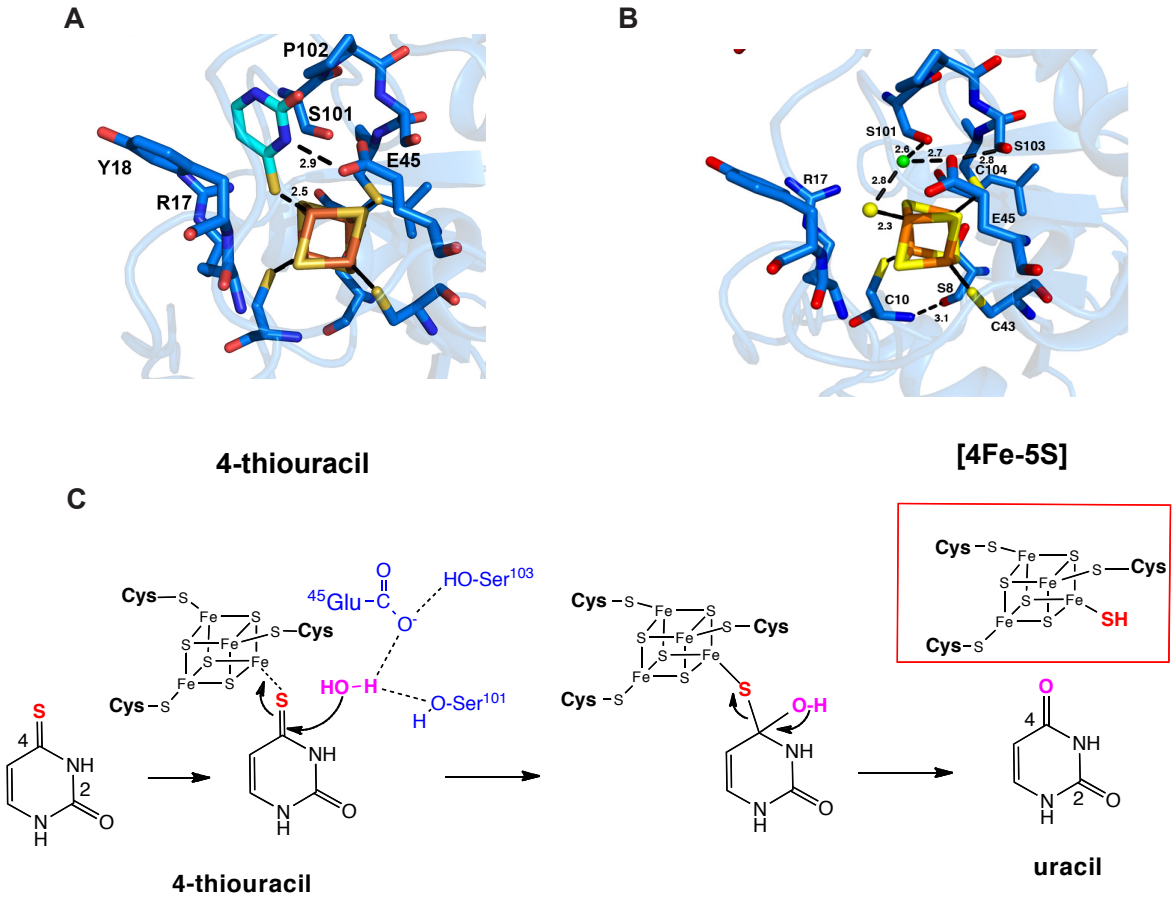

In the initial state, 4-thiouracil would bind to the cluster *via* its sulfur atom (Figure 3C, left), as shown by our docking studies (Figure 3A). We propose that a water molecule is located close the cluster/substrate complex, in a position equivalent to that observed in the structure containing the [4Fe-5S] cluster (Figure 3B). Such particular position, less than 3 Å away from both the fourth iron atom of the cluster and the sulfur atom of the substrate, seems indeed well designed to bind an exogenous heteroatom such as oxygen of ethylene glycol (Figure 1) or sulfur from a hydrosulfide ligand (Figure 2). This water molecule would be activated, thanks to H-bonds with Ser101 and Glu45, located 2.6 and 2.7 Å away, respectively, and become nucleophilic enough to attack the C-S bond of thiouracil. Indeed, Glu45 and Ser101 have been shown by site-directed mutagenesis to be catalytic residues. Nucleophilic substitution of the sulfur atom by hydroxide would be facilitated by the proximity of the cluster. The next step would involve the deprotonation of the hydroxyl group formed at the C4 atom of 4-thiouracil (Figure 3C, middle) and elimination of hydrosulfide, thus generating the [4Fe-5S] cluster

(Figure 3C, right). While not investigated here, the final step, that closes the cycle, necessitates the release of the S atom in solution to regenerate the [4Fe-4S] cluster. It is tempting to suggest that the adjacent water molecule provides the proton needed to release H_2S, in a reaction assisted by Glu45 (Figure 3B).

[4Fe-5S] clusters, with a cysteine ligand for three Fe atoms and a hydrosulfide ligand for the fourth Fe atom, have recently emerged as possible intermediates in sulfuration reactions involving iron-sulfur enzymes. This intermediate was proposed to be the actual S donor and thus to have the ability to transfer the fifth, exogenous, S atom to the activated substrate to be sulfurated in the case of tRNA-modifying enzymes such as U54-tRNA thiolase TtuA [12, 14] and methylthiotransferase MiaB, responsible for ms^2i^6A37 formation in tRNAs [29], as well for RimO, another methylthiotransferase introducing a thiomethyl group into a critical alanine of the ribosomal protein S12 [29]. Interestingly, the same intermediate has also been postulated earlier within the mechanism of L-cysteine desulfidase, an iron-sulfur enzyme involved in S mobilization from L-cysteine, most relevant to the chemistry of TudS [30].

However, in all these cases, the existence of the [4Fe-5S] cluster was postulated, but not unambiguously proven. In the case of TtuA from *Pyrococcus horikoshii*, the crystal structure displayed an extra electron density bound to the unique site of the cluster [12]. Although the chemical nature of the corresponding atom was not identified, it was consistent with a hydrosulfide ion. However, in that case, the putative [4Fe-5S] cluster was generated during chemical reconstitution of the cluster, in the presence of sulfide salts in excess, and not as part of the enzyme reaction. In the case of RimO, a crystal structure, also obtained after reconstitution of the cluster, showed a density attached to the cluster that was assigned to a polysulfide, reflecting the ability of the fourth Fe atom to bind a sulfide species [29].

Finally, the only [4Fe-5S] cluster that has previously been characterized by crystallography and anomalous scattering, is the cluster of the non-catalytic β-subunit of hydroxyisocaproyl-CoA dehydratase [20]. Although the structure of this enzyme is one of the most similar structures to that of TudS (Figure S9), the function of such [4Fe-5S] cluster in the β-cluster remains unknown as it is not connected to sulfur metabolism, and thus not relevant to the catalytic role of the [4Fe-5S] cluster in TudS.

CONCLUSION

In summary, we have reported here the first structural characterization of a [4Fe-5S] cluster catalytic intermediate, deriving from a physiologically relevant S transfer reaction from a sulfur donor, here a thiouracil substrate. This structure illustrates the novel function of iron-sulfur clusters as sulfur transfer agents. Such function of a [4Fe-4S] cluster as a Lewis acid [31] to bind and activate sulfur is reminiscent of the function of the [4Fe-4S] clusters in dehydration reactions catalyzed by enzymes such as aconitase [32]. The chemistry unraveled here is likely to apply to other desulfidase enzymes such as L-cysteine desulfidase [30], in which the enzyme would serve to transfer the S atom of L-cysteine to the cluster, or to sulfuration enzymes such as *Thermus thermophilus* TtuA, in which the enzyme would serve to transfer the S atom of the C-terminal thiocarboxylate of TtuB to the cluster [14]. In both cases, a [4Fe-5S] cluster would be formed, whose fate would depend on the enzyme. In the case of desulfuration reactions, hydrosulfide is liberated in solution, while in other cases, the activated hydrosulfide is used for sulfurating a second substrate, for example a uridine of a tRNA, as in the case of TtuA. Altogether, [4Fe-5S] clusters appear as the central active species in biological reactions involving sulfuration and desulfuration.

ACKNOWLEDGEMENTS

This work was supported by the French State Program 'Investissements d'Avenir' (Grants "LABEX DYNAMO", ANR-11-LABX-0011 and by the Research Council of Lithuania **(**Grant S-MIP-19-61). We acknowledge SOLEIL for provision of the synchrotron radiation facilities (proposal ID 20170872), and warmly thank Proxima 1 and Proxima 2 staff for assistance in using the beamlines. We thank the Macromolecular Interaction Platform of I2BC for use of its facilities and expertise and Christophe Velours for performing the SEC-MALS analysis.

REFERENCES

[1] H. Beinert, *Eur J Biochem* **2000**, *267*, 5657.
[2] E. Mulliez, V. Duarte, S. Arragain, M. Fontecave, M. Atta, *Front Chem* **2017**, *5*, 17.
[3] N. Shigi, *Front Genet* **2014**, *5*, 67.
[4] N. Shigi, *Front Microbiol* **2018**, *9*, 2679.
[5] O. Bimai, S. Arragain, B. Golinelli-Pimpaneau, *Curr Opin Struct Biol* **2020**, *65*, 69.
[6] K. A. Black, P. C. Dos Santos, *Biochim Biophys Acta* **2015**, *1853*, 1470.
[7] C. J. Fugate, J. T. Jarrett, *Biochim Biophys Acta* **2012**, *1824*, 1213.
[8] M. I. McLaughlin, N. D. Lanz, P. J. Goldman, K. H. Lee, S. J. Booker, C. L. Drennan, *Proc Natl Acad Sci U S A* **2016**.
[9] E. L. McCarthy, S. J. Booker, *Science* **2017**, *358*, 373.
[10] E. L. McCarthy, A. N. Rankin, Z. R. Dill, S. J. Booker, *J Biol Chem* **2019**, *294*, 1609.
[11] D. Bouvier, N. Labessan, M. Clemancey, J. M. Latour, J. L. Ravanat, M. Fontecave, M. Atta, *Nucleic Acids Res* **2014**, *42*, 7960.
[12] S. Arragain, O. Bimai, P. Legrand, S. Caillat, J. L. Ravanat, N. Touati, L. Binet, M. Atta, M. Fontecave, B. Golinelli-Pimpaneau, *Proc Natl Acad Sci U S A* **2017**, *114*, 7355.
[13] M. Chen, S. I. Asai, S. Narai, S. Nambu, N. Omura, Y. Sakaguchi, T. Suzuki, M. Ikeda-Saito, K. Watanabe, M. Yao, N. Shigi, Y. Tanaka, *Proc Natl Acad Sci U S A* **2017**, *114*, 4954.
[14] M. Chen, M. Ishizaka, S. Narai, M. Horitani, N. Shigi, M. Yao, Y. Tanaka, *Commun Biol* **2020**, *3*, 168.
[15] A. Aucynaite, R. Rutkiene, R. Gasparaviciute, R. Meskys, J. Urbonavicius, *Environ Microbiol Rep* **2018**, *10*, 49.
[16] H. Beinert, *Anal Biochem* **1983**, *131*, 373.
[17] W. W. Fish, *Methods in Enzymology* **1988**, *158*, 357.
[18] E. Krissinel, *J Comput Chem* **2010**, *31*, 133.
[19] E. Jurrus, D. Engel, K. Star, K. Monson, J. Brandi, L. E. Felberg, D. H. Brookes, L. Wilson, J. Chen, K. Liles, M. Chun, P. Li, D. W. Gohara, T. Dolinsky, R. Konecny, D. R. Koes, J. E. Nielsen, T. Head-Gordon, W. Geng, R. Krasny, G. W. Wei, M. J. Holst, J. A. McCammon, N. A. Baker, *Protein Sci* **2018**, *27*, 112.
[20] S. H. Knauer, W. Buckel, H. Dobbek, *Journal of the American Chemical Society* **2011**, *133*, 4342.
[21] J. H. Jeoung, H. Dobbek, *Proc Natl Acad Sci U S A* **2018**, *115*, 2994.
[22] L. Holm, *Protein Sci* **2020**, *29*, 128.
[23] A. Grosdidier, V. Zoete, O. Michielin, *Nucleic Acids Res* **2011**, *39*, W270.
[24] R. H. Lindsay, M. W. Yu, *Biochem Pharmacol* **1974**, *23*, 2273.
[25] J. A. Kiebooms, J. Wauters, J. Vanden Bussche, K. Houf, P. De Vos, S. Van Trappen, I. Cleenwerck, L. Vanhaecke, *Appl Environ Microbiol* **2014**, *80*, 7433.
[26] J. W. Bratzler, J. R. Barnes, R. W. Swift, *J Nutr* **1949**, *38*, 41.
[27] J. K. Heyes, D. Vaughan, *Proc. Roy. Soc. B.* **1967**, *169*, 89.
[28] J. M. Roux, *Enzyme* **1973**, *15*, 361.

[29] F. Forouhar, S. Arragain, M. Atta, S. Gambarelli, J. M. Mouesca, M. Hussain, R. Xiao, S. Kieffer-Jaquinod, J. Seetharaman, T. B. Acton, G. T. Montelione, E. Mulliez, J. F. Hunt, M. Fontecave, *Nat Chem Biol* **2013**, *9*, 333.
[30] S. I. Tchong, H. Xu, R. H. White, *Biochemistry* **2005**, *44*, 1659.
[31] D. H. Flint, R. M. Allen, *Chem Rev* **1996**, *96*, 2315.
[32] H. Beinert, M. C. Kennedy, C. D. Stout, *Chem Rev* **1996**, *96*, 2335.

Table of contents

[4Fe-5S] clusters are emerging as possible key catalytic intermediates in various sulfuration and desulfuration reactions. The structural characterization of a [4Fe-5S] intermediate coming from the transfer of a sulfur atom from thiouracil to the [4Fe-4S] cluster of an enzyme supports a novel function of [4Fe-4S] clusters as sulfur transfer agents.

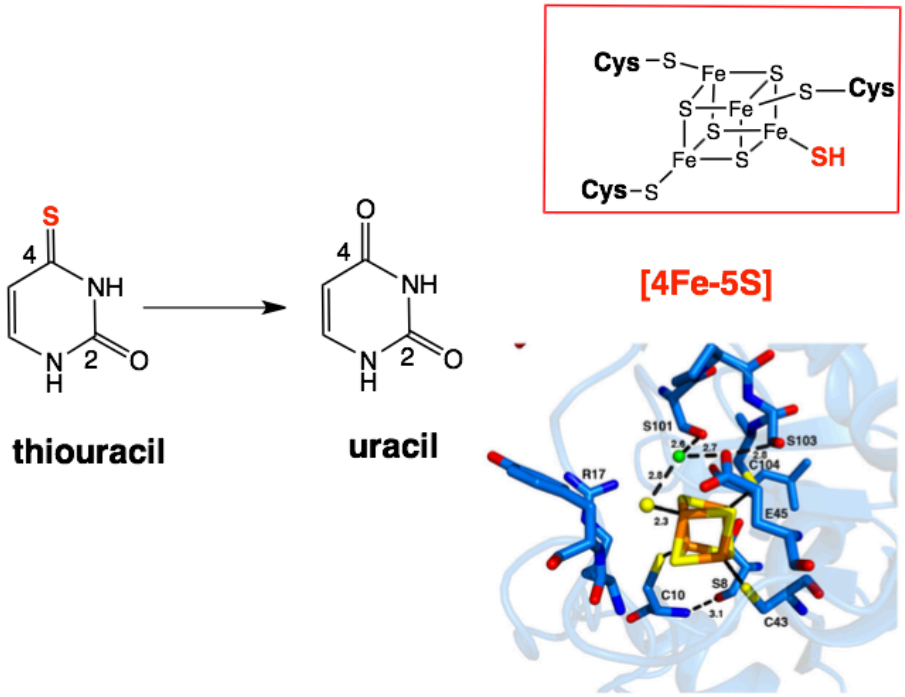

Keywords: cluster compounds, [4Fe-5S] cluster, desulfidase, enzyme catalysis, thiouracil

Supporting information. Table of contents: Experimental section, Supplementary Figures and Supplementary Table 1 (crystallographic statistics).

EXPERIMENTAL SECTION

Bacterial strains and plasmids

Escherichia coli DH5α (Thermo Fisher Scientific) was used for routine DNA manipulations. Aerobic expression of the *DUF523Vcz* gene was carried out in *E. coli* BL21(DE3) strain (Novagen). *E. coli* HMS174(DE3) (Novagen) was used for disruption of *pyrF* gene to obtain the HMS174Δ*pyrF* strain. The pET21b(+) vector (Novagen), which allows inducible expression of 6× His-tagged proteins at C-terminus, was used for cloning of the *DUF523Vcz* gene. Standard techniques were used for DNA manipulations [1].

Construction of *E. coli* HMS174Δ*pyrF* strain

The *pyrF* gene, which participates in the *de novo* synthetic pathway of uridine, was disrupted in the *E. coli* HMS174(DE3) strain using The Quick and Easy *E. coli* Gene Deletion Kit (Gene Bridges) according to technical protocol Version 2.3 (June 2012) using oligonucleotide primers *pyrF_FW_FRT* (5'-TTTACCTGTTTCGCGCCACTTCCGGTGCCCATCATCAAGAAGGTCTGGTCAATTAACCCT CACTAAAGGGCG-3') and *pyrF_RV_FRT* (5'-AATACGTCCGGTTTCCGTTGAGTAGACCAGACGGCTGTTGGAATCACTCATAATACGACT CACTATAGGGCTC-3'). The kanamycin selection marker was removed using the 708-FLPe expression plasmid (Gene Bridges) according to the manufacturer's protocol. DNA primers were synthesized at Metabion International AG.

In vivo activity of the TudS enzyme

The effect of the mutations on the activity of the TudS enzyme was tested *in vivo*. The uracil auxotrophic *E. coli* HMS174Δ*pyrF* cells, carrying either the wild-type or the mutated TudS encoding plasmid, were grown aerobically at 37 °C on M9 minimal medium supplemented with 100 μg/mL ampicillin, 0.1 mM IPTG, and 20 mg/L uracil, 2-thiouracil or 4-thiouracil as sources of uracil.

Cloning of the *DUF523Vcz* gene

The *DUF523Vcz* gene (GenBank accession number MG027705) was amplified by PCR using the *DUFVcz-pET21b-Fw* (5'-ATATACATATGAAGGAAAAAATCATAGTCAGCGCCTGC-3') and *DUFVcz-pET21b-Rv* (5'-TGGTGCTCGAGGGAGCCCGCTGCGGTGGCCACCAGGGAGAG-3') primers, digested with *Nde*I and *Xho*I (Thermo Fisher Scientific) restriction endonucleases and cloned into

the corresponding sites of pET21b(+) vector. DNA primers were synthesized by Metabion International AG. Correct insertion of the *DUF523Vcz* gene was confirmed by DNA sequencing.

Site-directed mutagenesis of TudS protein

Mutagenesis was carried out on plasmid pET21b(+)-*DUF523Vcz* using the QuikChange™ Lightning Multi Site-Directed Mutagenesis Kit from Agilent Technologies (US) according to the manufacturer's protocol. Oligonucleotide primers DUF R17A: 5'-CTGGGTCAGCCGGTAGCTTACGATGGCCAGAG-3', DUF R17K: 5'-CTGCTGGGTCAGCCGGTAAAGTACGATGGCCAGAGCA-3', DUF R17M: 5'-CTGCTGGGTCAGCCGGTAATGTACGATGGCCAGAGCA-3', DUF Y18A: 5'-GGGTCAGCCGGTACGTGCCGATGGCCAGAGC-3', DUF Y18F: 5'-GTCAGCCGGTACGTTTCGATGGCCAGAG-3', DUF Y18L: 5'-GGTCAGCCGGTACGTTTAGATGGCCAGAGCAAGG-3', DUF E45A: 5'-GTTCTGCCCCGCGGTGGCGGGCG-3', DUF E45D: 5'-TTCTGCCCCGATGTGGCGGGCGG-3', DUF E45Q: 5'-CGTTCTGCCCCCAGGTGGCGGGC-3', DUF K98A: 5'-GCTTTGCCCTGCTCGCGGAGGGGAGTCCCT-3', DUF K98L: 5'-CGCTTTGCCCTGCTCCTAGAGGGGAGTCCCTCC-3', DUF S101A: 5'-GCTCAAGGAGGGGGCTCCCTCCTGCGGC-3', DUF S101C: 5'-CTCAAGGAGGGGTGTCCCTCCTGCG-3', DUF S101T: 5'-TGCTCAAGGAGGGGACTCCCTCCTGC-3', DUF S103A: 5'-GAGGGGAGTCCCGCCTGCGGCAGTG-3', DUF S103C: 5'-GGGGAGTCCCTGCTGCGGCAGTG-3', DUF S103T: 5'-GAGGGGAGTCCCACCTGCGGCAGTG-3' were used. The mutations were confirmed by DNA sequencing.

Heterologous *DUF523Vcz* gene expression in *E. coli*

Bacterial cells were grown in LB medium, supplemented with 50 μg/mL ampicillin. Cells were incubated at 30°C until an optical density of 0.6–0.8 was reached. Expression of the *DUF523Vcz* gene was induced with 0.1 mM isopropyl β-D-1-thiogalactopyranoside (IPTG), and $FeSO_4$ was added to a final concentration of 20 μM. Cells were incubated for 18 h at 20°C with agitation of 120 rpm. Cells were harvested by centrifugation at 4 000× *g* (4°C) and used directly or stored at −80°C.

Aerobic purification of recombinant TudS protein

Purification procedures were carried out at 4 °C. Cells were resuspended in buffer A (50 mM Tris-HCl, pH 8 buffer, supplemented with 300 mM NaCl, 1.5 mM 2-mercaptoethanol, 1 mM phenylmethylsulfonyl fluoride (PMSF), and 10 mM imidazole). Cell suspension was disrupted by sonication using a VC-750 ultrasound processor (Sonics & Materials, Inc.). The cell lysate was centrifuged at 10,000 g for 1 h. Recombinant TudS protein was purified by a two-step procedure using an Äkta Purifier FPLC system (Amersham Biosciences). Cell extracts were loaded onto a 2 ml HisTrap™ HP column (GE Healthcare), previously equilibrated with buffer A without PMSF. After washing the column with 5 column volumes of equilibration buffer, the protein was eluted with a linear gradient of 10–400 mM imidazole in buffer A at 0.5 ml/min in 140 min. The colored fractions containing the TudS protein were analyzed on an SDS-PAGE gel, pooled and desalted using a 25 mL (5× 5 mL) HiTrap™ Desalting column (GE Healthcare), previously equilibrated with buffer B (25 mM Tris-HCl buffer pH 8, containing 1.5 mM 2-mercaptoethanol). The protein was then loaded onto a 1 mL HiTrap™ Q XL column (GE Healthcare), previously equilibrated with buffer B. After washing the column with 5 column volumes of buffer B, TudS was eluted using a linear gradient of 0–600 mM NaCl in buffer B at 0.8 ml/min in 30 min. The fractions containing the highest concentration of TudS were pooled and desalted using a 25 mL (5× 5mL) HiTrap™ Desalting column, previously equilibrated with buffer B. After checking the purity by electrophoresis on a 12% SDS-PAGE gel, the recombinant protein was concentrated by ultrafiltration using a 10 kDa cut-off membrane (Millipore).

[Fe-S] cluster reconstitution and purification of holo-TudS

The reconstitution of the [4Fe-4S] cluster and purification of holo-TudS were performed under strict anaerobic conditions in an Mbraun glove box containing less than 0.5 ppm O_2. After incubation of 100 µM as-purified TudS with 10 mM dithiothreitol for 10 min, a 5.5-fold molar excess of ferrous ammonium sulfate and L-cysteine as well as 2 µM *E. coli* cysteine desulfurase CsdA were added, and incubation was extended overnight. After centrifugation for 30 min at 20,000g, holo-TudS was loaded onto a Superdex 200 10/300 increase gel filtration column (GL Sciences) equilibrated in 20 mM Tris pH 8.0 buffer. The peak containing holo-TudS was collected then concentrated to 7 mg/ml on a Vivaspin concentrator (10 kDa cutoff).

The concentration of recombinant TudS was measured using Bradford method [2] with bovine serum albumin as the calibration standard.

SEC-MALS analysis

Size Exclusion Chromatography coupled with Multi-angle light scattering (SEC-MALS) experiments were performed using an HPLC-MALS system (Shimadzu) equipped with static light scattering detector (mini DAWN TREOS, Wyatt Technology), refractive index detector (Optilab T-rEX, Wyatt Technology) and UV detector (SPD-20A, Shimadzu). holo-DUF (100 µl at 2mg/ml) was injected on a Superdex 200 10/300 GL increase column (GE Healthcare) equilibrated in 50 mM Tris-HCL pH 7.5, 200 mM NaCl buffer at a flow rate of 0.5 $ml.min^{-1}$. Molar masses of proteins were calculated using the ASTRA 6.1 software (Wyatt Technology) using a refractive index increment (dn/dc) value of 0.183 $ml\ g^{-1}$.

Enzymatic activity measurements

Enzymatic activity tests were carried out under anaerobic conditions (95% N_2, 5% H_2) and analyzed by Ultra performance liquid chromatography (UPLC). The reaction mixtures containing 100 mM MOPS/KOH pH 7.3 buffer, 0–1000 µM 4-thiouracil or 2-thiouracil and 0–25 µM of recombinant TudS enzyme were incubated at 30 °C for 30 s in a total volume of 50 µL. Reactions were started by adding the enzyme and stopped by adding 5 µL of formic acid. Supernatants were analyzed on an Acquity H Class UPLC (Waters) by reversed-phase chromatography (Waters Acquity UPLC HSS T3 2.1×100 mm column, 1.8 µm particle size). For separation, a gradient of water/acetonitrile with 0.1% formic acid was used. The identity of substrates and products were determined by their retention time and spectra and their concentrations in comparison to the standards.

Crystallization, Data Collection, and Structure Determination

Holo-TudS at 3.6 mg/mL was crystallized under anaerobic conditions using the sitting drop procedure by mixing 1 µL protein with 1 or 2 µL reservoir solution containing 10 mM $MgCl_2$, 0.1 M MES, pH 5.5, 7–9% PEG 6000 at 293 K. Crystals appeared after 5–6 days. Crystals were cryoprotected with the crystallization solution supplemented with 20% v/v ethylene glycol and flash-frozen under anaerobic condition using liquid propane. X-ray diffraction data were collected at 100 K on single crystals at Proxima-1 and Proxima-2 beamlines at the synchrotron SOLEIL (Saint-Aubin, France). Data were indexed, processed, merged and scaled using autoPROC [3-6]. Data used for substructure solution and refinements were all from the STARANISO analysis within the autoPROC pipeline. The structure was solved by single-wavelength anomalous dispersion using the anomalous signal of the iron of the iron-sulfur

cluster. A partial substructure consisting of two iron superatoms was first found with SHELXC/D [7] using data at 3.2 Å resolution. The substructure was then completed using Phaser-EP [8] using the heavy atoms sites found with SHELX and searching for two [4Fe-4S] clusters at 3.2 Å resolution. The resulting sites were given as input to autoSHARP [9, 10]. The final map of autoSHARP was clearly interpretable and was used as input in Phenix.autobuild [11], which generated a model with 287 residues out of 332 for two subunits with Rwork/Rfree of 0.26/0.33. Model completion was performed by alternating manual building in COOT [12] and refinement with autoBUSTER (version 2.11.1) using NCS restraints [13].

Several TudS crystals were soaked under anaerobic conditions in crystallization buffer containing 15 mM 4-thiouracil for 5-15 minutes. Crystals were then cryoprotected using the same cryo protecting buffer complemented with 15 mM 4-thiouracil, flash frozen in liquid propane, then stored in liquid nitrogen until X-ray diffraction analysis. Diffraction data were collected at one or more photon energies (12.67 keV for native data, 7.125 keV for phasing at the Fe edge and 6.5 keV for detecting the sulfur anomalous signal), depending on the size of the crystal, with at least 20 μm of unexposed region between collection spots to account for diffusion of free radicals.

Crystal 1 was used for solving the structure using the Fe anomalous signal, crystals 2 and 3 for refinement at high resolution and for identifying the sulfur atoms around the [4Fe-4S] cluster site, crystals 4 and 5 for detecting the sulfur and iron atoms at the [Fe-S] site after soaking with the 4-thiouracil substrate. Data processing and refinement statistics are summarized in Tables S1 & S2. The volume of the active site pocket was determined with HOLLOW [14] and calculated with ChimeraX [15].

Modeling studies

Docking thiouracil/thiouridine derivatives was carried out with EADock, which is provided on the Swissdock web server [16]. Missing hydrogens in the TudS crystal structure were added using the "Structure editing/AddH" tool in UCSF CHIMERA [17]. The program was used in the default fast protocol. The clusters are classified according to the fullfitness energy (Table S3).

Supplementary Figures

Figure S1. Sequence alignment of several putative TudS proteins. Alignment of *Aeromonas* TudS with Q45584 from *Bacillus subtilis*, D6B003 from *Streptomyces albidoflavus*, A0A653B309 from *Pseudomonas oleovorans*, A0A0H3GN09 from *Klebsiella pneumoniae*, WP_004083256.1 from *Thermotoga maritima*, WP_012940503.1 from *Archaeoglobus profundus* and A0A0A2WIY4 from *Beauveria bassiana* was performed with Clustal Omega [18] and rendered with *ESPript* [18]. All proteins contain three conserved cysteines (indicated as dots) that ligate the [4Fe-4S] cluster in *Aeromonas* TudS.

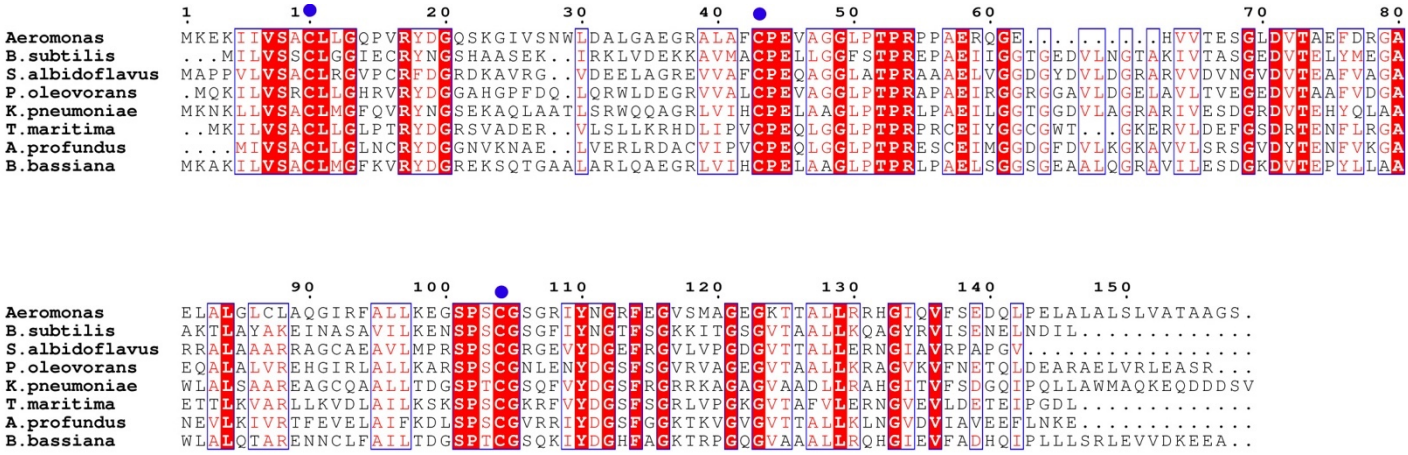

Figure S2. Enzymatic activity of *Aeromonas* TudS. *In vivo* functionality of wild-type and various TudS mutants analyzed by complementation of the HMS174Δ*pyrF* strain in the presence of various uracil compounds. WT (wild-type) corresponds to the *DUF523vcz* gene in pET21b(+). The empty vector was used as a negative control. The following TudS mutants were analyzed: R17A, R17K, R17M, Y18A, Y18F, Y18L, E45A, E45D, E45Q, K98A, K98L, S101A, S101C, S101T, S103A, S103C, S103T. Minimal medium (M9) was used as a negative control. It was supplemented with either 20 mg/L 2-thiouracil (M9 + 2-TU), 4-thiouracil (M9 + 4-TU) or uracil (M9 + U; positive control).

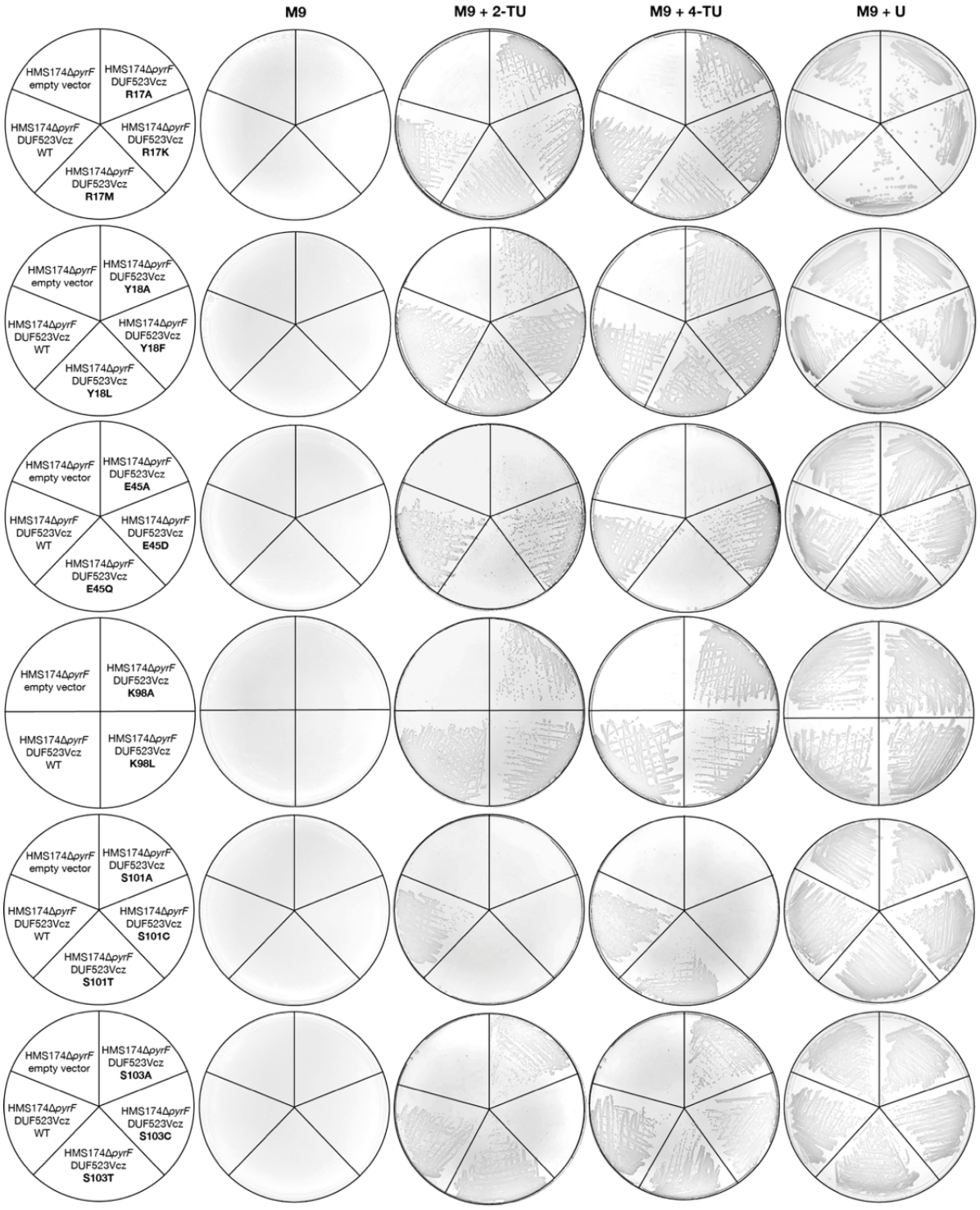

Figure S3.

A 12% SDS-PAGE gel of as-purified TudS. **B** Chromatographic profile of holo-TudS after cluster reconstitution and anaerobic purification on a Superdex 200 increase 10/300 GL column. The pooled fractions are framed. **C** SEC-MALS analysis of holo-TudS. Holo-TudS (2 mg/ml) was loaded onto a Superdex 200 10/300GL increase column equilibrated with 50 mM Tris-HCl pH 7.5, 200 mM NaCl. Plot of the relative refraction index (dashed black line), light diffusion signal (full black line), absorbance at 410 nm (dotted black line) and weighted-average molar mass (red line) as a function of elution volume. The measured molar mass of 16.3 ± 5.2 kDa corresponds to the monomer (theoretical molar mass of 17.6 kDa). **D** UV-visible spectrum of 45 µM holo-TudS in 20 mM Tris-HCl, pH 8.

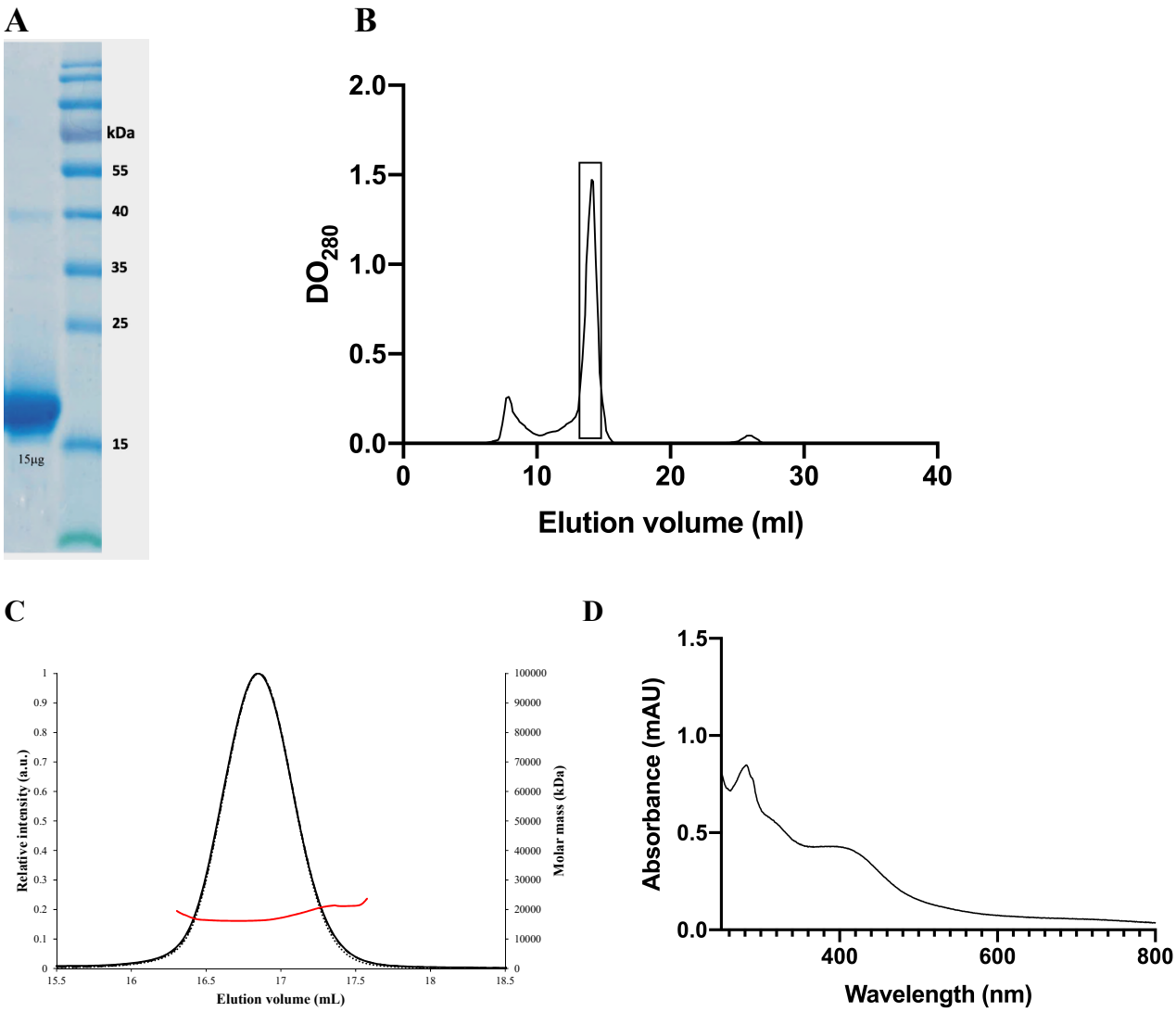

Figure S4. *In vitro* dethiolation of 2-thiouracil and 4-thiouracil by TudS. 50 µM TudS was incubated with 500 µM 2-thiouracil (1–4) and 4-thiouracil (5–8) for 0 min (1, 5), 1 min (2, 6), 5 min (3, 7), 15 min (4, 8) at 30 °C anaerobically and the substrates/products were analyzed by UPLC. Both substrates are converted into uracil. Retention times: uracil, 2.4 min (green), 2-thiouracil, 3.7 min (blue), 4-thiouracil, 5.7 min (orange).

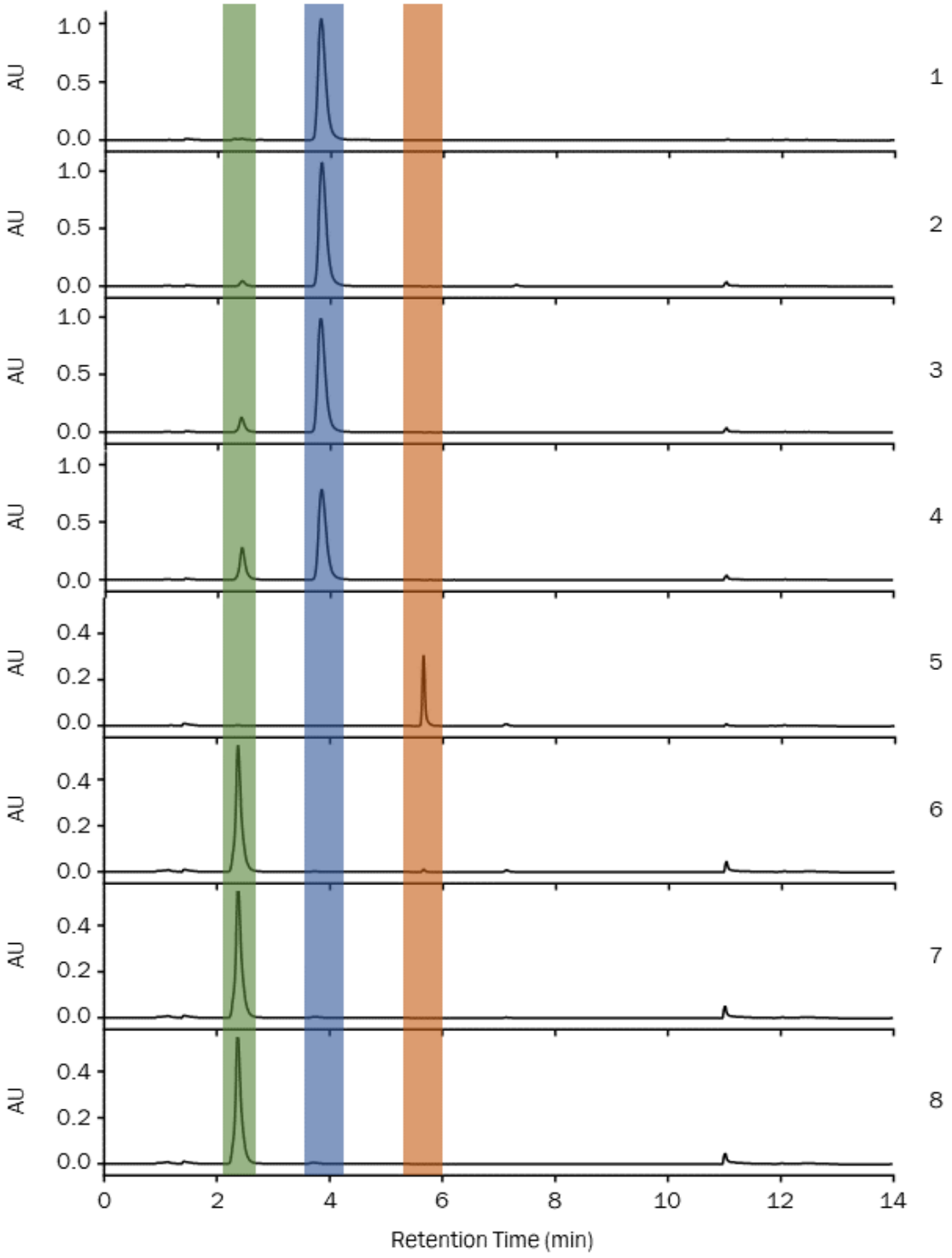

Figure S5. Crystal structure of non-soaked TudS crystal. **A** View of the two molecules in the asymmetric unit of TudS crystal 2, represented as ribbons, the diameter of which increases with the B-factors (colored from blue to red for the range 14-50 Å^2). **B** Superposition of the two molecules in the asymmetric unit (in cyan and green; rmsd of 0.11 Å for 117 Cα atoms) with residues next to the cluster in stick representation. **C** Stereoview of ethylene glycol bound to the cluster of TudS. Fo-Fc and 2Fo-Fc maps omitting ethylene glycol and polyethylene glycol are contoured at the level of 3 σ (green) and 1 σ (black), respectively.

A

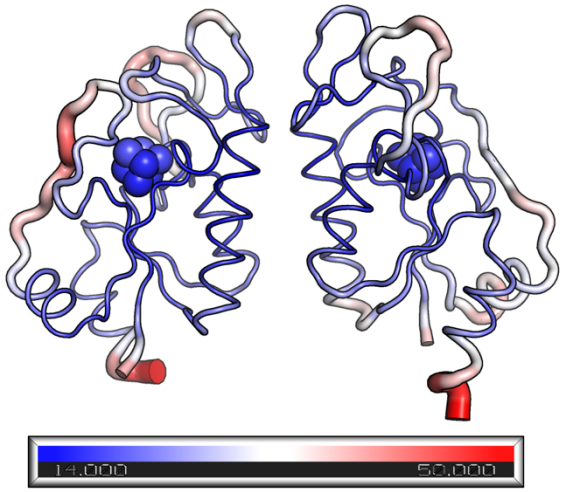

B

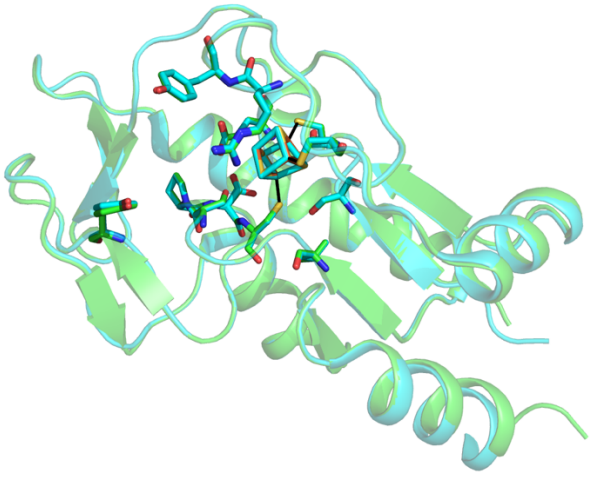

C

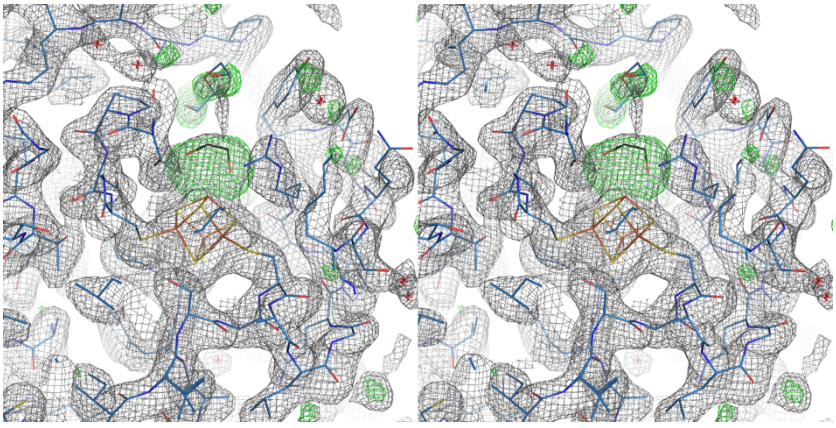

Figure S6. Position of the sulfur atom attached to the cluster in the two molecules of TudS crystals soaked with 4-thiouracil. **A** Stereoview of the [4Fe-5S] cluster site in molecule A (crystal 5). Fe and S anomalous difference maps for data collected at 7.125 and 6.5 keV, are shown in green and magenta, respectively, and contoured at 3.5 σ. **B** The fifth sulfur atom bound to the [4Fe-4S] cluster adopts two distinct positions in molecule B, with relative occupancies 0.67/0.33. The anomalous difference map for data collected at 6.5 keV for sulfur detection is contoured at the level of 3.5 σ. **C** Environment of the cluster in molecule B of the TudS crystal (same orientation as Figure 2B).

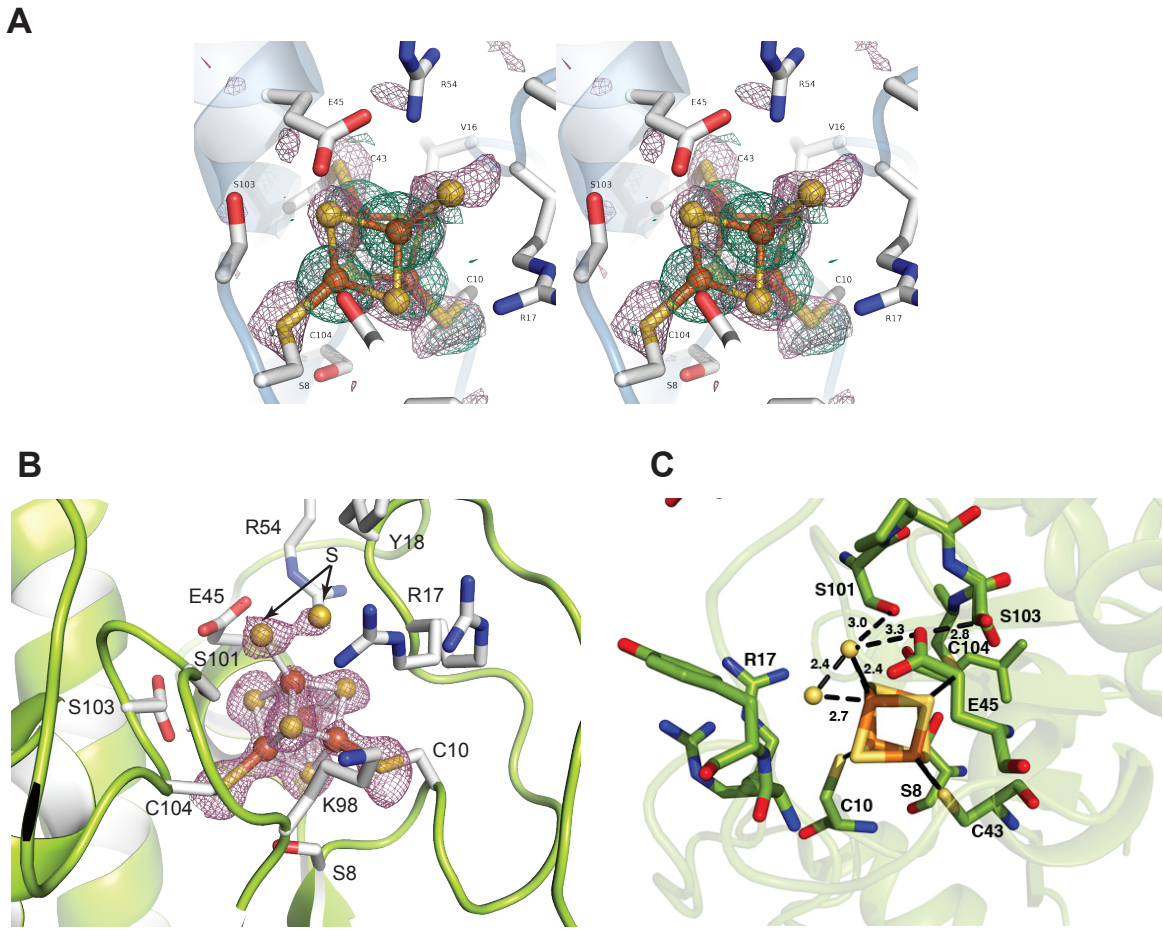

Figure S7. Comparison of the angles formed between each Fe-S bond within the cluster and the bond linking the Fe atom and the external sulfur-containing ligand for TudS, HadC (PDB 3O3M) and DCCP (PDB 6ENO).

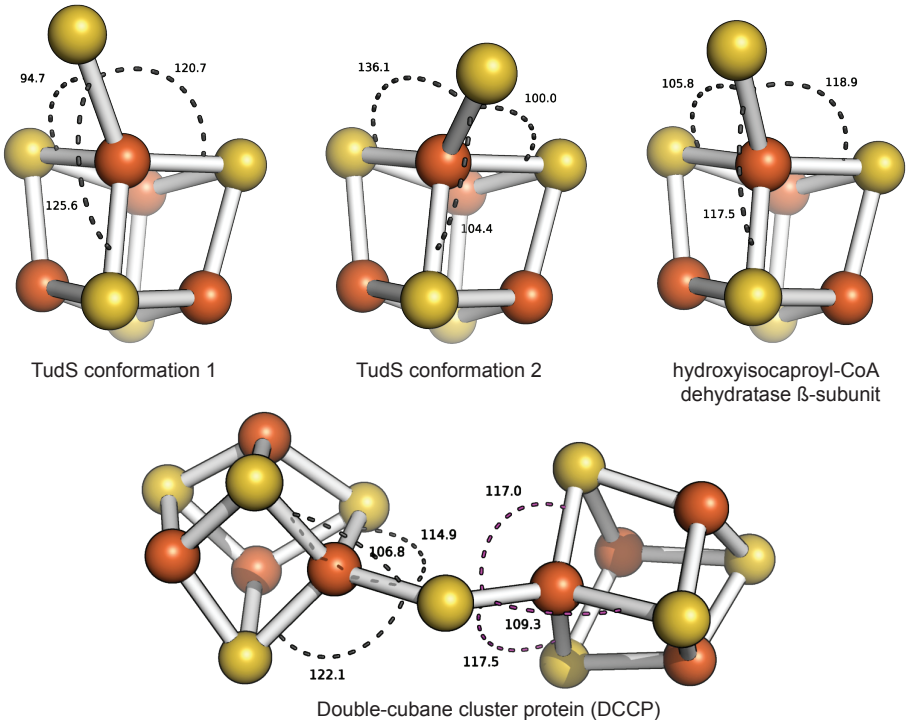

Figure S8. Comparison of the angles that makes the bond between one Fe atom of the [4Fe-4S] cluster and a sulfur-containing ligand, external to the [4Fe-4S] cluster (e.g. L-cysteine from the protein) with the three internal Fe-S bonds of the cluster (see Figure S7 for illustration). All [4Fe-4S]-containing structures in the PDB solved at a resolution better than 1.45 Å (118 structures at the time of analysis) were analyzed with PYMOL. Angles are defined as angle 1 ≤ angle 2 ≤ angle 3 with symbols for Tuds conformation 1 (blue circle), Tuds conformation 2 (magenta square), HadC (green triangle), DCCP cluster 1 (cyan diamond) and DCCP cluster 2 (red diamond). **A, B** and **C** show the distributions in bins of 1 degree obtained for the three angles. **D** is a boxplot representation of the same data.

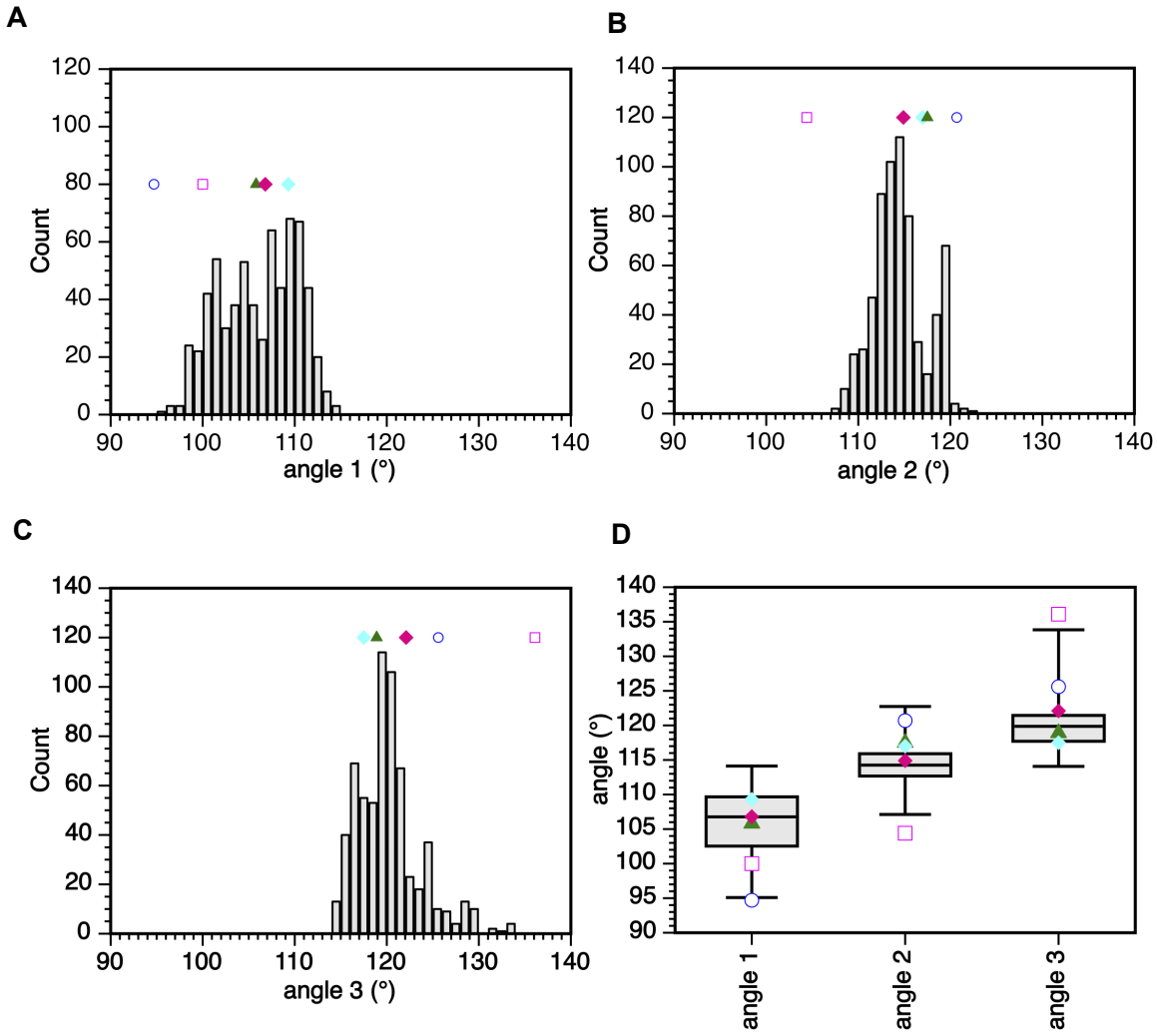

Figure S9. Comparison of TudS and 2-hydroxyisocaproyl-CoA dehydratase. **A** Stereo view of TudS (in blue) and HadC (PDB code 3O3M, in green) after superposition with DALI. The [4Fe-5S] clusters are shown as spheres (orange for iron, yellow for sulfur atoms for TudS and green for HadC. **B** Comparison of the [4Fe-5S] clusters of TudS (left) and HadC (right). The cavity around the cluster, as detected by PYMOL in cavity mode with default settings, is shown as a grey mesh.

A

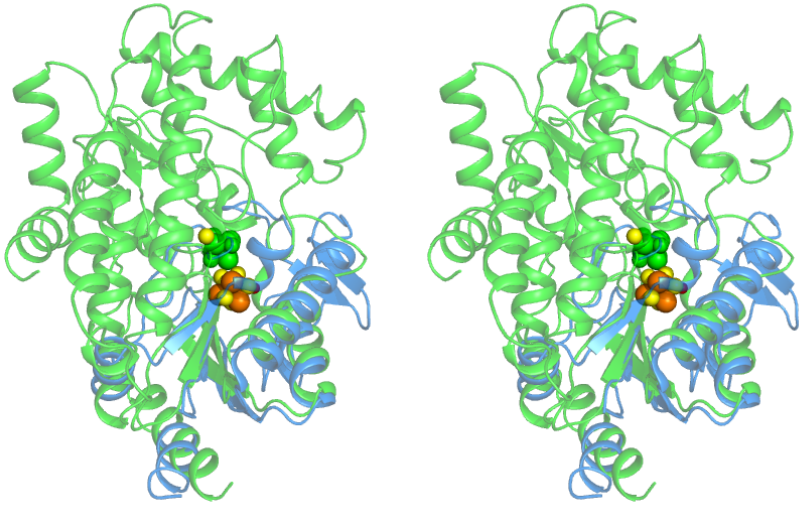

B

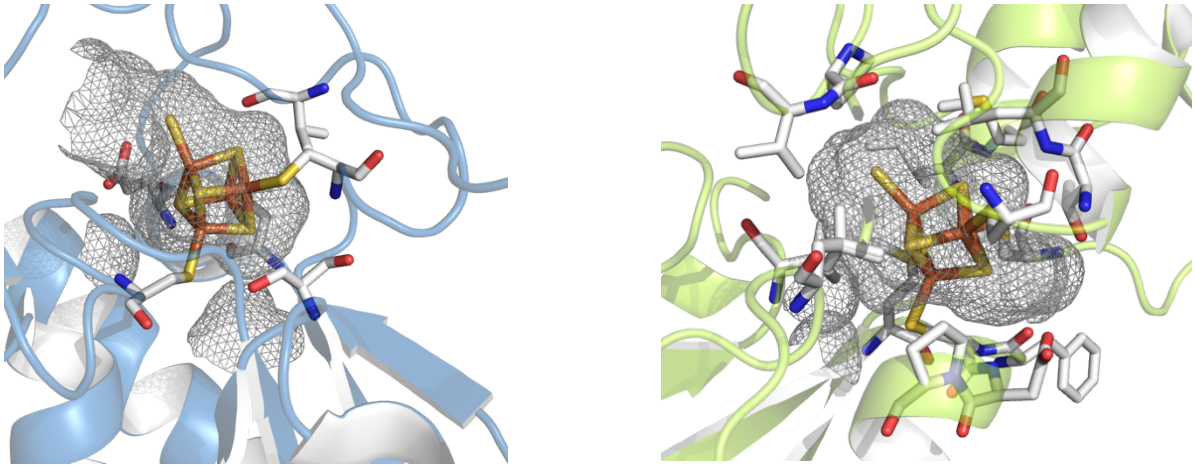

Figure S10. Models of 2-thiouracil and 4-thiouracil bound to TudS, as calculated with Swissdock. The two best conformations are shown. Hydrogen bonds within 3.2 Å are shown as dashed lines with the number indicating the distance in Å.

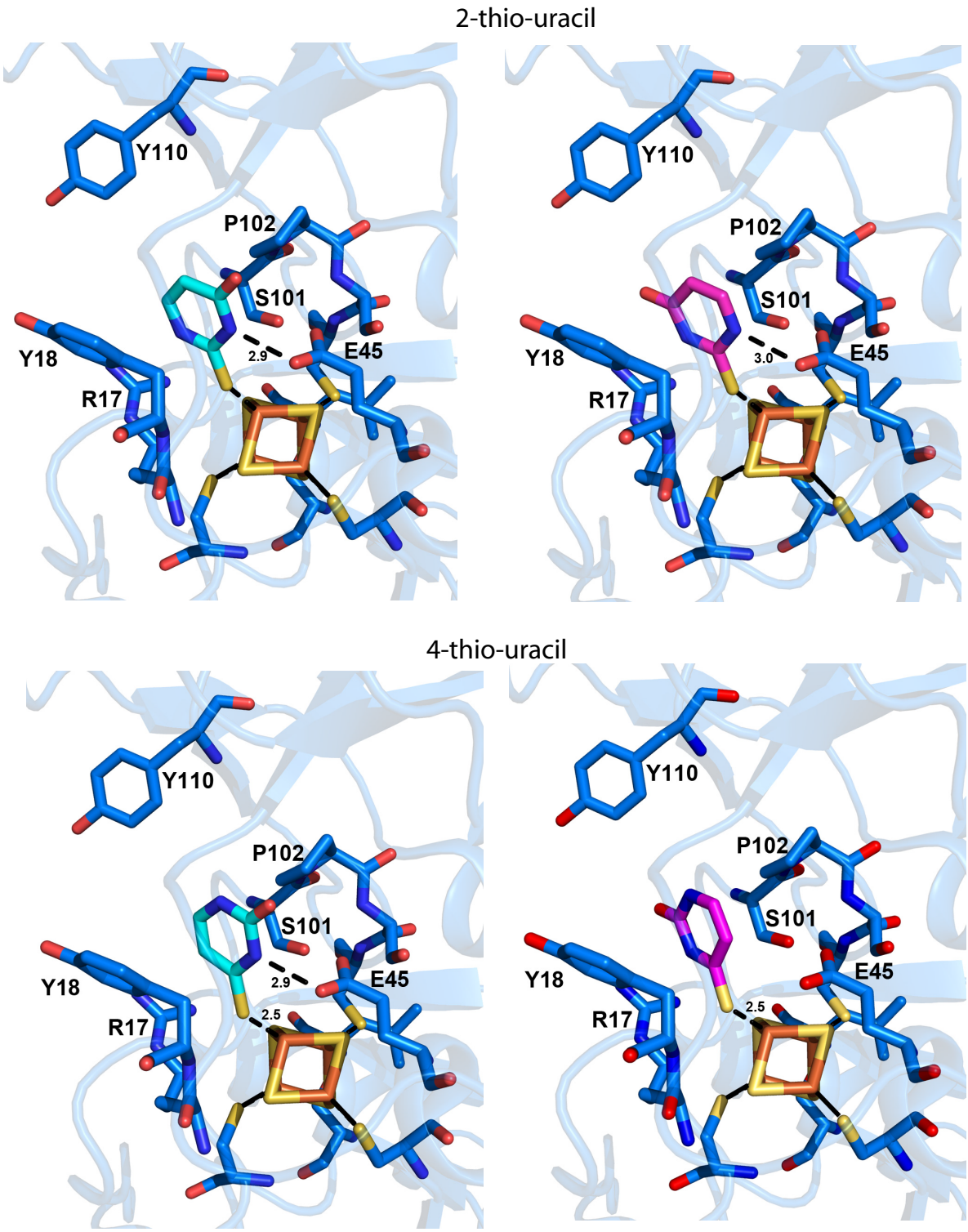

Table S1 Summary of data collection and refinement statistics. Crystal 1 was used for solving the structure using the Fe anomalous signal, crystals 2 and 3 for refinement at high resolution and for identifying the sulfur atoms around the [4Fe-4S] cluster site, crystals 4 and 5 for detecting the sulfur and iron contents at the [Fe-S] site after soaking with the 4-thiouracil substrate.

A Statistics for non-soaked TudS crystals

	Crystal 1[1]		Crystal 2			Crystal 3
PDB code[2]	6Z92			6Z93		6Z94
Data collection						
Beamline	Proxima 1	Proxima 1	Proxima 2	Proxima 2	Proxima 2	Proxima 1
Photon energy (keV)	7.125 iron edge	12.670 native	12.650 native	6.500 sulfur detection	7.125 Iron edge	6.500 sulfur detection
Space group	C2			C2		C2
Cell dimensions						
a, *b*, *c* (Å)	133.403, 86.040, 39.750	133.280, 85.911, 39.565	134.381, 85.812, 39.512	134.278, 85.494, 39.525	134.461, 85.706, 39.568	133.759, 85.797, 39.444
α, β, γ (°)	90.00, 93.62, 90.00	90.00, 93.64, 90.00	90.00, 93.92, 90.00	90.00, 93.94, 90.00	90.00, 93.95, 90.00	90.00, 93.88, 90.00
Resolution (Å)	72.26 – 2.43 (2.60 – 2.43)	66.51 – 2.07 (2.30 – 2.07)	72.27 – 1.50 (1.70 – 1.50)	72.07 – 2.01 (2.17 – 2.01)	72.22 – 1.83 (1.99 – 1.83)	66.73 – 1.76 (1.91 – 1.76)
R_{sym} or R_{merge}	0.202 (2.329)	0.143 (1.260)	0.093 (1.147)	0.152 (1.055)	0.134 (0.939)	0.093 (1.346)
R_{meas}	0.211 (2.530)	0.161 (1.421)	0.10 (1.24)	0.161 (1.244)	0.132 (1.160)	0.097 (1.472)
$I / \sigma I$	11.3 (0.9)	7.6 (1.4)	10.9 (1.7)	10.6 (1.3)	11.3 (1.3)	15.3 (1.0)
Completeness (%)						
spherical	78.6 (22.3)	70.0 (13.9)	59.4 (9.3)	77.1 (18.9)	75.3 (17.0)	69.9 (15.6)
ellipsoidal	85.7 (35.3)	89.8 (41.9)	89.5 (56.9)	85.8 (33.5)	85.8 (35.1)	86.3 (43.5)
No. unique reflections	13255	18587	42459	23027	29698	30836
Redundancy	12.2 (6.7)	4.5 (4.5)	6.8 (7.0)	9.6 (3.2)	9.6 (3.5)	12.6 (6.1)
CC(1/2)	0.994 (0.182)	0.991 (0.310)	0.998 (0.488)	0.994 (0.505)	0.997 (0.562)	0.999 (0.486)
Refinement						
Resolution (Å)	-	66.51 – 2.07	29.03-1.50	-	-	72.17 – 1.76
No. reflections	-	18594	42447	-	-	30837
R_{work} / R_{free}	-	0.195 / 0.220	0.168 / 0.194	-	-	0.183 / 0.207
No. atoms	-			-	-	
Protein	-	2210	2227	-	-	2212
Ligand/ion	-	43	54	-	-	65
Water	-	124	299	-	-	272
B-factors	-			-	-	
Macromolecule	-	38.21	26.09	-	-	33.01
Ligand/ion	-	38.45	33.73	-	-	39.99
Water	-	38.93	43.78	-	-	48.82
R.m.s. deviations	-			-	-	
Bond lengths (Å)	-	0.008	0.008	-	-	0.008
Bond angles (°)	-	0.92	0.93	-	-	0.92
Ramachandran	-					
Favored (%)	-	97.98	99.33			98.65
Allowed (%)	-	2.02	0.67	-	-	1.35
Outliers (%)	-	0.00	0.00	-	-	0.00
Molprobity Clashscore		4.21	1.71	-	-	2.99

[1] Each data set was collected from a single crystal.
[2] The PDB includes map coefficients, anisotropically treated data with Staraniso and isotropically treated data without resolution cut-off applied.

B Statistics for TudS crystals soaked with 4-thiouracil

	Crystal 4	Crystal 5		
PDB code	6ZW9		6Z96	
Data collection				
Beamline	Proxima 1	Proxima 2	Proxima 2	Proxima 2
Photon energy (keV)	6.500 sulfur detection	12.650 native	6.500 sulfur detection	7.125 Iron edge
Space group	C2		C2	
Cell dimensions				
a, *b*, *c* (Å)	136.165, 85.519, 39.576	134.666, 85.776, 39.515	134.638, 85.613, 39.414	134.865, 85.698, 39.454
α, β, γ (°)	90.00, 94.01, 90.00	90.00, 94.10, 90.00	90.00, 94.11, 90.00	90.00, 94.09, 90.00
Resolution (Å)	42.76 – 1.76 (1.85 -1.76)	39.69 – 1.33 (1.50 - 1.33)	67.15 – 2.02 (2.15 - 2.02)	67.26 – 1.86 (1.97 – 1.86)
R_{sym} or R_{merge}	0.081 (0.253)	0.077 (1.151)	0.088 (0.542)	0.095 (0.599)
R_{meas}	0.086 (0.283)	0.084 (1.26)	0.090 (0.591)	0.100 (0.713)
$I / \sigma I$	18.9 (4.0)	12.2 (1.5)	26.8 (3.6)	18.1 (2.1)
Completeness (%)				
spherical	88.4 (34.8)	67.6 (11.1)	79.2 (24.1)	79.6 (26.4)
ellipsoidal	91.2 (40.4)	92.2 (53.1)	84.7 (29.9)	84.7 (31.7)
No. unique reflections	39587	69773	23215	29872
Redundancy	9.6 (4.6)	6.8 (6.0)	23.0 (6.5)	9.8 (3.2)
CC(1/2)	0.997 (0.955)	0.998 (0.548)	0.998 (0.737)	0.998 (0.636)
Refinement				
Resolution (Å)	24.12 – 1.76	39.69 – 1.33	-	-
No. reflections	39569	69773	-	-
R_{work} / R_{free}	0.168 / 0.189	0.165 / 0.184	-	-
No. atoms			-	-
Protein	2226	2236	-	-
Ligand/ion	33	44	-	-
Water	412	333	-	-
B-factors			-	-
Macromolecule	15.11	23.16	-	-
Ligand/ion	17.98	27.61	-	-
Water	31.52	40.10	-	-
R.m.s. deviations			-	-
Bond lengths (Å)	0.008	0.008	-	-
Bond angles (°)	0.91	0.96	-	-
Ramachandran				
Favored (%)	99.00	99.01	-	-
Allowed (%)	1.00	0.99	-	-
Outliers (%)	0.00	0.00	-	-
Molprobity Clashscore	2.57	0.63	-	-

Table S2: Angles measured between the internal Fe-S bonds of the cluster and the bond between the fourth iron atom and the fifth inorganic sulfur atom for TudS, HadC and DCCP.

	TudS conformation 1	**TudS conformation 2**	**hydroxyisocaproyl-CoA dehydratase ß-subunit**	**Double-cubane cluster protein**
Angle 1	94.7 (-2.73)	100.0 (-1.46)	105.8 (-0.07)	106.8 (0.17) /109.3 (0.77)
Angle 2	120.7 (2.17)	104.4 (-3.55)	117.5 (1.04)	114.9 (0.13) / 117.0 (0.87)
Angle 3	125.6 (1.59)	136.1 (4.66)	118.9 (-0.38)	122.1 (0.56) / 117.5 (-0.79)

In parentheses, the Z-score obtained from the survey of the PDB for the structures deposited with a d_{min}< 1.45 Å and containing a [4Fe-4S] cluster.

Table S3. Molecular docking scores for thiouracil substrates.

Ligand	FullFitness (kcal/mol)[a]	Estimated ΔG[b] (kcal/mol)	d C(S)[c]-E45 OE1 (Å)	d C(S)- S101 O1G (Å)
2-thiouracil (cluster0, conf 1)	-792.43	-6.46	3.7	4.4
2-thiouracil (cluster1, conf 2)	-791.11	-6.55	3.7	4.5
4-thiouracil (cluster0, conf 1)	-792.00	-6.49	3.8	4.6
4-thiouracil (cluster5, conf 1)	-787.81	-6.29	3.9	4.7

[a] The FullFitness of a cluster is calculated by averaging the 30% most favorable effective energies of its elements, in order to limit the risk of a few complexes penalizing the whole cluster. This effective energy is the sum of the total energy of the system and a solvation term.
[b] interaction energy, as calculated by EADock
c C (S) designs the carbon atom that bears the sulfur atom: C2 or C4
"conf" stands for "conformation"

[1] J. Sambrook, D. W. Russell, *Molecular Cloning: a laboratory manual.*, New York Cold Spring Harb. Lab. Press, **2001**.
[2] M. M. Bradford, *Anal Biochem* **1976**, *72*, 248.
[3] C. Vonrhein, C. Flensburg, P. Keller, A. Sharff, O. Smart, W. Paciorek, T. Womack, G. Bricogne, *Acta Crystallogr D Biol Crystallogr* **2011**, *67*, 293.
[4] W. Kabsch, *Acta Crystallogr D Biol Crystallogr* **2010**, *66*, 125.
[5] P. R. Evans, G. N. Murshudov, *Acta Crystallogr D Biol Crystallogr* **2013**, *69*, 1204.
[6] P. Evans, *Acta Crystallogr D Biol Crystallogr* **2006**, *62*, 72.
[7] I. Uson, G. M. Sheldrick, *Acta Crystallogr D Struct Biol* **2018**, *74*, 106.
[8] A. J. McCoy, R. W. Grosse-Kunstleve, P. D. Adams, M. D. Winn, L. C. Storoni, R. J. Read, *Journal of Applied Crystallography* **2007**, *40*, 658.
[9] C. Vonrhein, E. Blanc, P. Roversi, G. Bricogne, *Methods Mol Biol* **2007**, *364*, 215.
[10] T. C. Terwilliger, P. D. Adams, R. J. Read, A. J. McCoy, N. W. Moriarty, R. W. Grosse-Kunstleve, P. V. Afonine, P. H. Zwart, L. W. Hung, *Acta Crystallogr D Biol Crystallogr* **2009**, *65*, 582.
[11] D. Liebschner, P. V. Afonine, M. L. Baker, G. Bunkoczi, V. B. Chen, T. I. Croll, B. Hintze, L. W. Hung, S. Jain, A. J. McCoy, N. W. Moriarty, R. D. Oeffner, B. K. Poon, M. G. Prisant, R. J. Read, J. S. Richardson, D. C. Richardson, M. D. Sammito, O. V. Sobolev, D. H. Stockwell, T. C. Terwilliger, A. G. Urzhumtsev, L. L. Videau, C. J. Williams, P. D. Adams, *Acta Crystallogr D Struct Biol* **2019**, *75*, 861.

[12] P. Emsley, B. Lohkamp, W. G. Scott, K. Cowtan, *Acta Crystallogr D Biol Crystallogr* **2010**, *66*, 486.
[13] O. S. Smart, T. O. Womack, C. Flensburg, P. Keller, W. Paciorek, A. Sharff, C. Vonrhein, G. Bricogne, *Acta Crystallogr D Biol Crystallogr* **2012**, *68*, 368.
[14] B. K. Ho, F. Gruswitz, *BMC Struct Biol* **2008**, *8*, 49.
[15] T. D. Goddard, C. C. Huang, E. C. Meng, E. F. Pettersen, G. S. Couch, J. H. Morris, T. E. Ferrin, *Protein Sci* **2018**, *27*, 14.
[16] A. Grosdidier, V. Zoete, O. Michielin, *Nucleic Acids Res* **2011**, *39*, W270.
[17] E. F. Pettersen, T. D. Goddard, C. C. Huang, G. S. Couch, D. M. Greenblatt, E. C. Meng, T. E. Ferrin, *J Comput Chem* **2004**, *25*, 1605.
[18] P. Gouet, E. Courcelle, D. I. Stuart, F. Metoz, *Bioinformatics* **1999**, *15*, 305.